

# A REVIEW OF AERONAUTICAL FATIGUE INVESTIGATIONS IN SWEDEN DURING THE PERIOD MAY 2007 TO APRIL 2009



EDITED by HANS ANSELL  
Saab Aerosystems  
Sweden

ICAF Doc. No. 2419



## CONTENTS

3.1	Introduction.....	3
3.2	Investigations on operational events .....	4
3.2.1	Accident with a CASA C-212 aircraft during maritime patrol operation. ....	4
3.2.2	In-service cracking of parts belonging to the nacelle installation of Saab 2000 .....	7
3.2.3	Flight control system induced loading [2].....	9
3.3	Structural evaluation .....	12
3.3.1	The Saab 2000 Full Scale Fatigue Test and Damage tolerance Test.....	12
3.3.2	Wing/fuselage fatigue test.....	12
3.3.3	Saab 2000 Verification of structural repairs with respect to additional authority requirements.....	16
3.3.4	JAS39 Gripen Fatigue Testing.....	17
3.3.5	Continuing fatigue testing of the single seater, 39A .....	17
3.3.6	Full scale fatigue test of the twin seater export version, 39D .....	17
3.3.7	Export Standard Pylons Fatigue Tests.....	19
3.3.8	Refuelling Transfer Units Fatigue Tests.....	21
3.4	Fatigue crack initiation and propagation .....	23
3.4.1	A Case Study of Multiple-Site Fatigue Crack Growth in the F-18 Hornet Bulkhead.....	23
3.4.2	Crack growth simulation for stiffened panels [5].....	25
3.4.3	Validation of Damage Tolerance Analytical Models [6].....	27
3.4.4	Stress Intensity Factors for Multiple Surface Cracks [7].....	30
3.4.5	Decreasing fatigue properties of thick aluminum plate .....	32
3.4.6	Residual life prediction based on inspections [8].....	33
3.5	Composite materials .....	34
3.5.1	Effects of CFRP laminate thickness on the bending after impact strength .....	34
3.5.2	Fatigue Test for Impact Damage Growth Threshold in Composite Laminates under Variable .....	36
	Amplitude Loading Conditions.....	36
3.5.3	Characteristics of Lamb wave in detecting damages in composite materials [9].....	37
3.6	References.....	39
3.7	Acknowledgements.....	39

### 3.1 INTRODUCTION

In this paper a review is given of the work carried out in Sweden in the area of aeronautical fatigue during the period May 2007 to April 2009. The review includes basic studies of fatigue development in metals and composites, stress analysis and fracture mechanics, studies of crack initiation and propagation and residual strength, testing of full-scale structures, and fatigue life predictions. A reference list of relevant papers issued during the period covered by the review is included.

Contributions to the present review are from the following bodies:

- The Swedish Defence Research Agency (FOI), Aeronautics Division, FFA  
Sections 3.4.1, 3.4.2, 3.4.3, 3.4.4, 3.5.2, 3.5.3
- SAAB Aerosystems  
Sections 3.2.2, 3.2.3, 3.3.1, 3.3.2, 3.3.3, 3.3.4, 3.3.5, 3.3.6, 3.3.7, 3.3.8, 3.4.5, 3.5.1 and 3.5.2
- The Swedish Accident Investigation Board (SHK)  
Sections 3.2.1
- Chalmers University (CTH)  
Sections 3.4.6

## 3.2 INVESTIGATIONS ON OPERATIONAL EVENTS

### 3.2.1 Accident with a CASA C-212 aircraft during maritime patrol operation.

In the previous Swedish ICAF review [1] a fatal accident with a CASA C-212-CE aircraft was reported. The aircraft was operated by the Swedish Coast Guard in a maritime patrol role and during a low by-pass over the harbour bay the aircraft suddenly lost control after separation of the left side wing and crashed into the sea. At the time of the accident, the aircraft had accumulated 17,000 flight hours and 7,300 flight cycles. A full investigation, conducted by the Swedish Accident Investigation Board, was immediately initiated.



Figure 1. CASA-212-CE aircraft in maritime patrol operation.

After initial examination of the evidences, cracks, suspected to be caused by fatigue, were found in the centre wing lower skin at STA Y=1030. The lower wing skin at this station has an external doubler riveted to wing skin consisting of 6 rivet rows. The cracks were confined to the first rivet row in the skin where the external doubler ends. The cracking was wide spread extending over a large portion of the wing chord, figure 2. Cracks were also found in the same area of the right hand side wing.

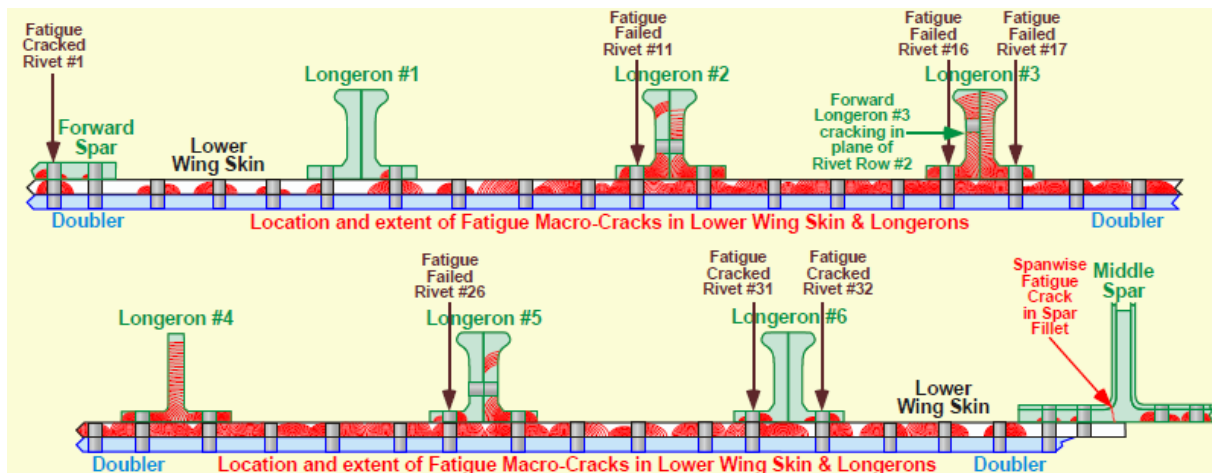


Figure 2. Schematic fatigue crack pattern in the left wing skin at STA Y=1030.

Cracks were found not only at the row of holes but also at the adjacent area following the existing grinding marks (Production standard of C-212 aircraft).



*Figure 3. Typical crack pattern, cracks following existing grinding marks.*

The investigation of the cause of the accident has been ongoing in close cooperation with consultants to the Swedish Accident Investigation Board and the Spanish aircraft manufacturer EADS CASA. The investigation proceeded in three main directions:

- The history of the accident aircraft, investigations regarding operations, repairs as well as any incidents in the past.
- The design of the wing and its load carrying principles and stressing.
- The maintenance system applied.

#### 1. Inspection for cracks in other C-212 aircraft

About 1/3 of the fleet of the aircraft type have been inspected. Various methods have been applied in these inspections ranging from simple to more advanced techniques on some aircraft. At this point no cracks have been found in this area in any other aircraft (however, broken rivets have been found in the critical row in some a/c).

#### 2. Investigation of the operation of the aircraft in maritime patrol service and in similar low altitude operations.

The accident aircraft has been operated within its envelope, no systematic exceedances have been reported. Pilots have been interviewed confidentially and log files checked, no overloads reported. The sister aircraft (having the same operational role and the about the same total flight time) has a reported overload but no similarities regarding the cracking. On minor difference is that the accident aircraft has been used in pilot training more extensively than the sister aircraft (short and hard landings, one engine flight phases). Both aircraft perform normally hard turns on low altitudes and in turbulent air. Manoeuvres to negative loadfactors followed by high positive are common (roller coast manoeuvres).

### 3. Local stresses wing lower skin including local bending.

At the cracked row, there is a fairing connecting the wing to the fuselage aimed to carry thrust loads in the aircraft longitudinal direction, figure 4. The design of this fairing is however also supposed to transfer some vertical loads which partly may have contributed to the cracking by induced bending in the failed section. Fatigue cracked rivets give evidence of such an assumption.

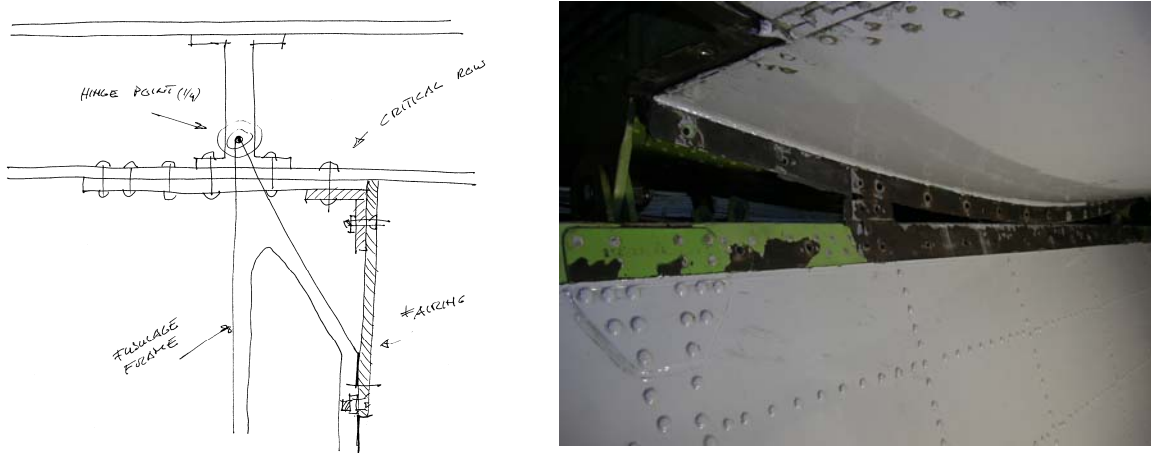


Figure 4. Sketch showing the principle of wing to fuselage fairing and a photo showing the position.

The manufacturer EADS CASA is performing a structural test program with coupons and panels with the parameters which could have had an influence on crack initiation (type of rivet, sealant, scratches, fairing induced load, etc.).

Using different types of coupons, the effect of the sealant and surface roughness of the fatigue strength have been evaluated. No detrimental effect of the surface roughness obtained with the standard grinding process used on the C-212 compared to "normal roughness" of 2024-T3 clad sheet product surface was found. The tensile fatigue strength of the 3.2 mm and 4.0 mm rivets has also been evaluated by testing. Coupons prestressed in compression were also tested but showed only a slight reduction in fatigue life, abt. 20%.

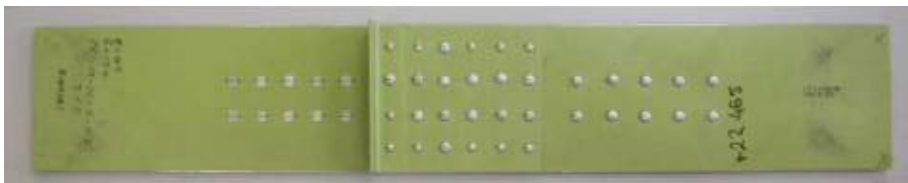


Figure 5. Coupon simulating the skin panel + doubler + stringer joint.

The panel tests are not yet completed.

### 4. A flight test program to measure the loads introduced by the wing-fuselage fairing.

The stress measurements flight test plan is divided in: flight test, fuel filling test (with fuselage fairing installed and removed) and test with unbalanced propeller (left and right propeller unbalanced). The flight tests have

The measurements show that the wing to fuselage fairings carry part of the wing vertical load. Also, a local stress increase at this area due to the secondary bending is found. This secondary bending is due to the "hard point" effect of the doubler and the fairing load. These findings were based on fuel filling tests and flight test with manouvres to just above 2 g. The tests with unbalanced propeller did not show any significant effect on stress amplitudes.

The investigation is not completed. The final report to be issued by the Swdish Accident Investigation Board regarding the probable cause of the accident has not been released.

### 3.2.2 In-service cracking of parts belonging to the nacelle installation of Saab 2000

For some years ago, a primary structural element associated with the engine installation to Saab 2000 was found be cracked on aircraft in service. See figure 6 for location of the subject item.

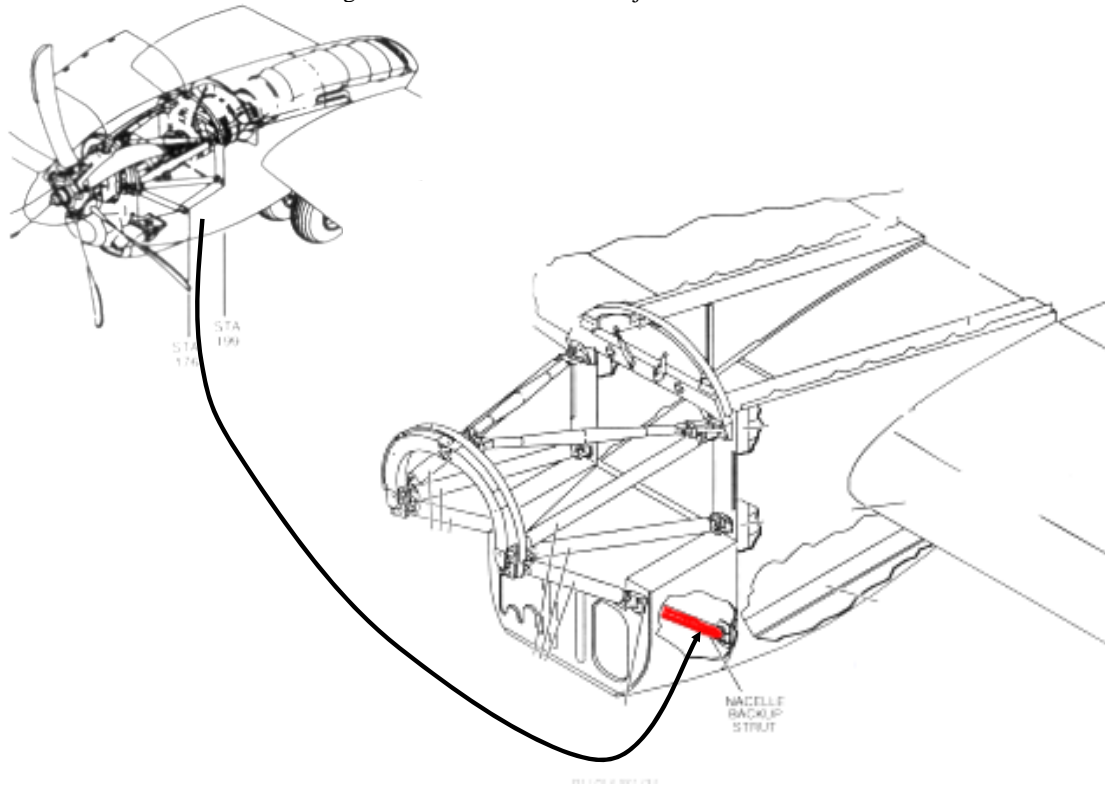


Figure 6 Primary Structural element –Welded design

The strut is made from titanium with integrated attachments welded to the tube. The critical location from fatigue point of view is located at the ends where the welded portion interferes with the cut out for the attachment fitting. Consequently, this zone was subjected to cracking on Aircraft in service caused by loading (mass, gust and manoeuvre loads) from the engine transferred to the nacelle. Cracks started from the cut out were discovered at several strut as depicted in figure 7.

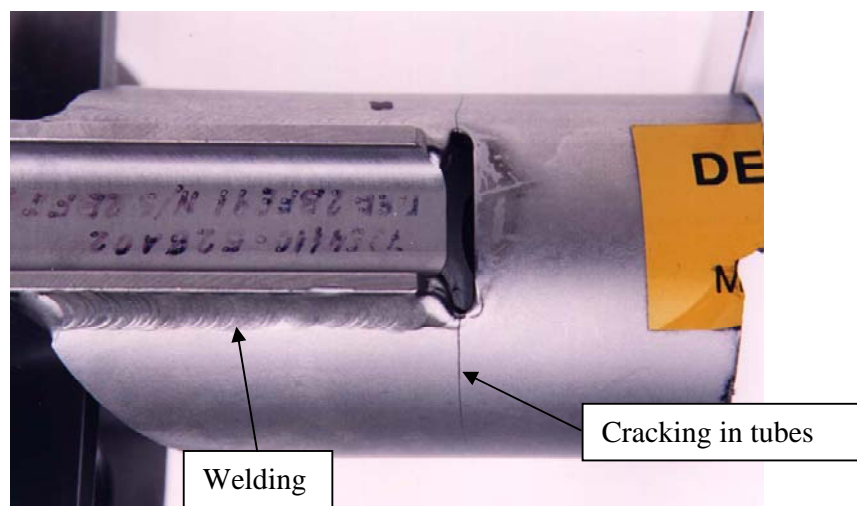


Figure 7. Welded attachment to the strut

The results from the investigation concluded that the crack propagation on the struts was significant higher than the crack growth analysis. The correlated crack growth curve based on metallurgical examinations (striations) was derived according to figure 8. Diamond shaped symbols (◆) represent the point of time for findings on aircraft in service.

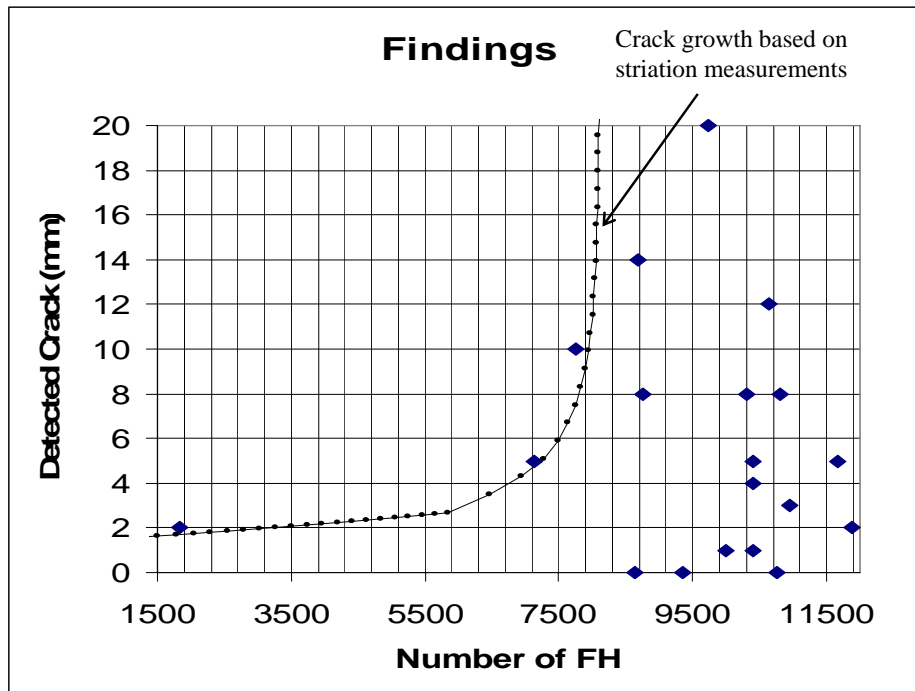


Figure 8. Correlated crack growth curve based on findings on aircraft in Service

Summarizing, the struts were afflicted with several discrepancies causing the major extent of the cracking. These were as follows :

- Major portion of residual stresses in the tube due to welding
- Multiple stress concentrations- from cut out and end of welding (interaction)
- Presence of initial flaws/pittings in the tube due to pickling operation

Figure 9 outlines the strut installed on the Full scale fatigue test together with a strut from an aircraft in service. The strut installed on the test specimen was not subjected to any crack growth during the complete testing, however the local design of the strut was different compared to aircraft in service. The cut out and the welded portion was not interfered to each other as on struts mounted on aircraft in service. Hence, a more propitious design was obtained leading that no cracks occurred in the test.



Figure 9 Comparison of details around the cut out

### 3.2.3 Flight control system induced loading [2]

Modern generation combat aircraft have several features and duties that make individual aircraft tracking more crucial than ever before. Multi-role capacity will lead to aircraft that will encounter a larger variability in fatigue loading. The digital flight control system will also generate fatigue loading not present in aircraft having less complex control systems. One of the advantages of a digital flight control system is also the ability to improve aircraft performance after the aerodynamic and structural designs are complete. This flexibility of the system will be utilised when tactical advantages can be gained. Such revisions can bring both advantages and disadvantages for the airframe structure in terms of damage tolerance and durability.



Figure 10. Control surfaces on a modern fighter aircraft.

The loads monitoring system of Gripen makes information for investigations into certain interesting flight conditions easily accessible. A flight phase which may increase the severity of the cyclic loading of canards, is flying in close formation. The aircraft, flying behind another aircraft, may encounter turbulent air generated by the lead aircraft. The flight control system will react on this disturbance through small and frequent canard movements. In the left part of figure 11 the measured canard rotation angles are shown for both the lead aircraft (blue curve) and for the aircraft flying immediately behind (red curve).

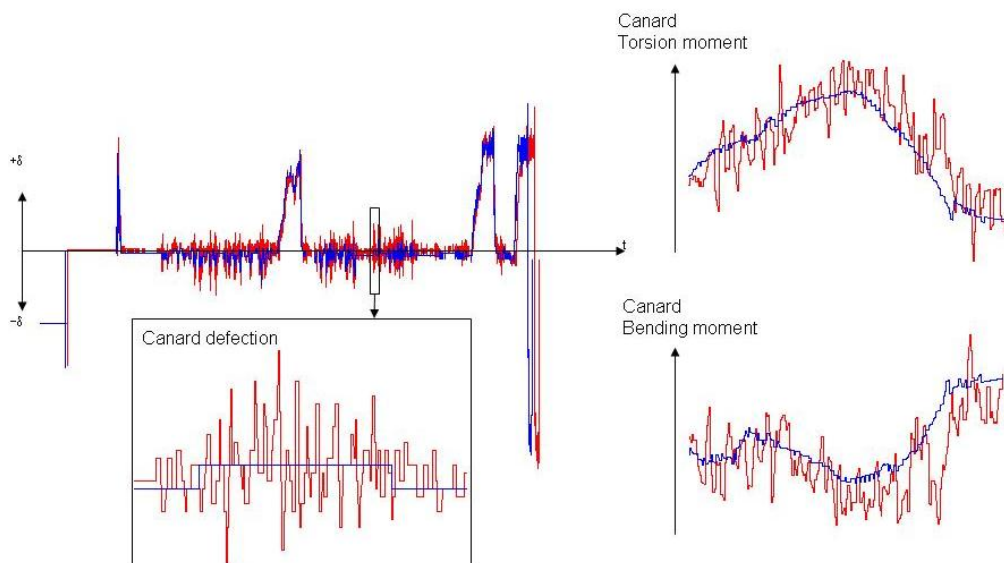


Figure 11. Left part - Canard rotation angles during close formation flying. Right part - calculated torsion and bending moments in the canard. Blue curves are for lead aircraft and red curves are for the second aircraft

The frequent movements will result in bending and torsion moments in the surrounding structure. The magnitude of the moments depends on several other flight conditions such as speed, altitude, angle of attack, load factor etc. and can be calculated using aerodynamic and flight mechanics models of the aircraft, see the right part of figure 11. The consequence in terms of fatigue life, that these load fluctuations have on the airframe, depends on the specific design of the canard installation. The canards in Gripen are attached to the fuselage through a pivot axle to an outer and inner beam. The movements of the pivot axle are generated by a duplex servo actuator, see the left part of figure 12.

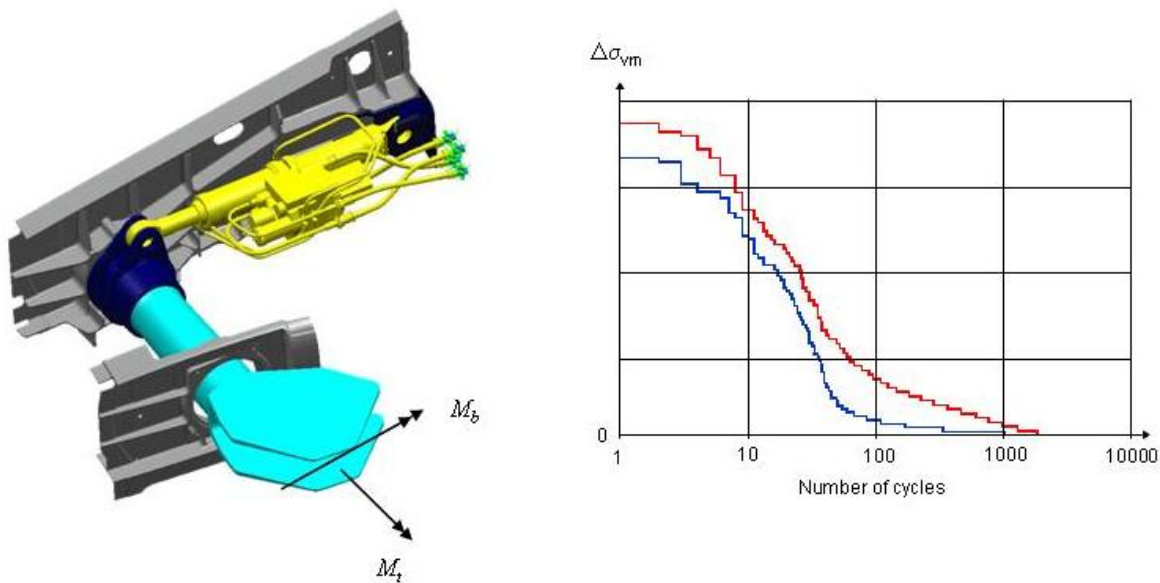


Figure 12. Left part - the pivot for the attachment of the canard. Right part - von Mises stress range spectra. Blue curve is for lead aircraft and red curve is for the second aircraft

The torsion and bending of the pivot axle will generate a biaxial stress state at the surface of the pivot. Bending and torsion moment sequences have been calculated for the complete flight for both lead aircraft and the aircraft flying behind. The von Mises stress on the surface of a round bar is proportional to the torsion moment  $T$  and the bending moment  $M$  through  $(4M^2 + 3T^2)^{1/2}$ . This relation has been used to calculate stress spectra in terms of von Mises stress for both lead and the second aircraft as compared in the right part of figure 12. The relative life factor, of the canard pivot, between the two aircraft depends on the stress level but is typically 2 at stress levels which should result in a life limitation for a typical fighter design life (the actual stress is far below that level in Gripen).

The above investigation was initiated after indications of many small cycles in some flight conditions from the loads monitor system. The analysis of the strain signals, both in terms of torsion and bending moment calculations as well as cycle counting according to the rain-flow algorithm, is done on-line during flight. In order to check the effect of close formation flying further, an individual aircraft which has been used in close formation training has been selected. The rain-flow matrix for the torsion moment was extracted from the period of interest as well as the median rain flow matrix for the complete fleet of aircraft for all time. In order to make fatigue tests with these two spectra, reconstructions of the load sequences were necessary. The reconstructions were made using algorithms which produce a time sequence which will give exactly the same rain-flow matrix as it was derived from. The testing was done using coupon specimens of aluminium AA7010 and furnished with a central open hole and an electro-spark machined flaw at the edge of the hole. The stress level in the test with the median spectrum was selected to result in a slow crack growth life regime typical for a fighter aircraft, i.e. 10000 flh. The crack growth life of the specimens subjected to the spectrum as obtained from the aircraft flying in close formation training was about 2.3 times shorter, i.e. in the same regime as for the calculated example given above, see results shown in figure 13.

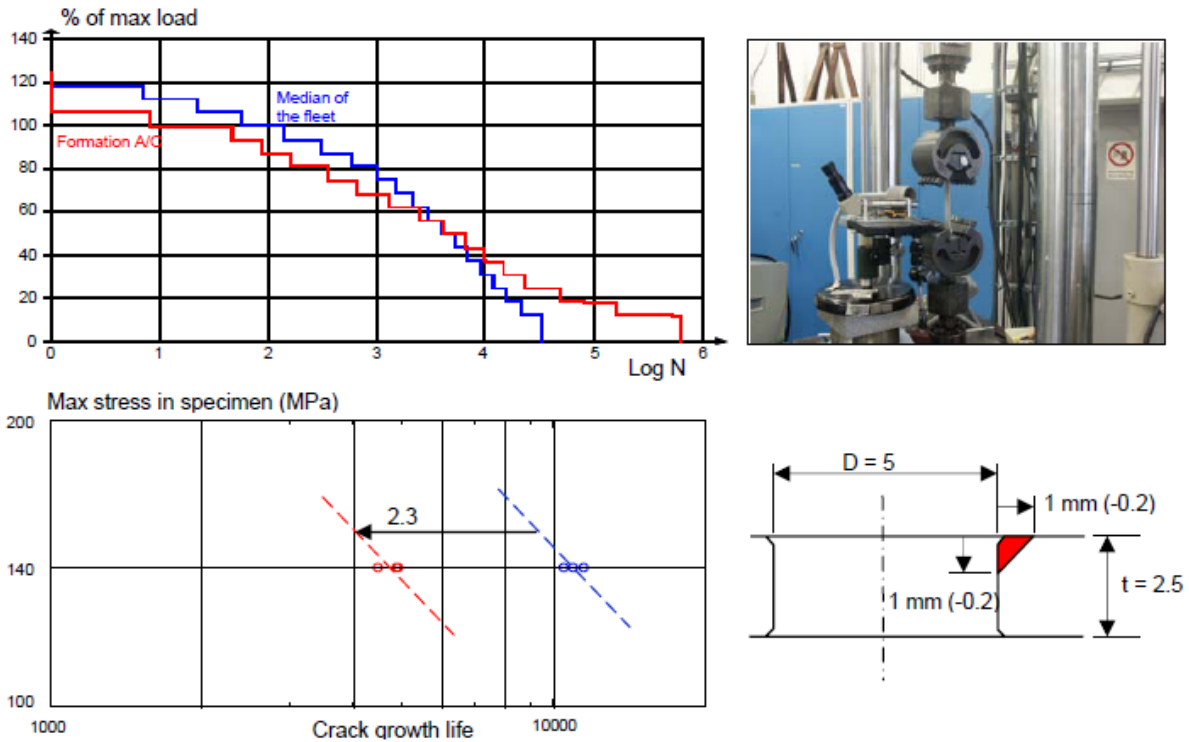


Figure 13. Comparison of crack growth life in fatigue testing using a median spectrum for the fleet (blue curves) and monitored data obtained from an individual aircraft in close formation training (red curves).

Another structural part that is affected in close formation flight is the actuator for the canard control. This actuator induces the canard rotation by acting on the flight control system commands. An actuator for a primary control surface consists of a redundant electro-mechanical control servo, hydraulic tandem actuator and triplex position sensors for the main control valve and the actuator, respectively. This configuration enables the aircraft, after failure detection and reconfiguration, to be flown and landed with one or even two of the primary servos or control surfaces failed. There are, however, some parts of the actuators that are classified as critical parts, and calls for a damage tolerance assessment, since a failure may cause the control surface to come loose and induce flutter.

A key factor in the damage tolerance analysis is the pressurization spectrum for each of the chambers in the actuators. It has turned out that the pressure pulsations induced by the flight control system can be more damaging than actuator loads for manoeuvring. The most damaging cycles are those which arise from chamber pressure fluctuations due to small control surface movements e.g. as in close formation flying. An additional complication is present for the duplex servos since “force-fighting” between the two systems can occur. Both the pressure fluctuations and the force-fighting originate from imperfections in the servo valve which control both systems. Valve parameters such as mean pressure, pressure amplification, radial clearance, un-symmetry, combinations of overlap etc. in combination with small sliding movements have a great effect on the pressure fluctuations. Thus, the chambers of the actuators are subjected to large number of low and medium range pressure cycles. These may have a considerable effect on the crack growth rate if they exceed the threshold range.

### 3.3 STRUCTURAL EVALUATION

#### 3.3.1 The Saab 2000 Full Scale Fatigue Test and Damage tolerance Test

The Design Service Goal (DSG) for Saab 2000 is presently 75000 flights or 60000 flight hours whichever occurs first. For the Saab 2000, no complete airframe will be tested due to the commonality with the Saab 340. Consequently, a number of full scale component tests are used to justify the long term characteristics.

#### 3.3.2 Wing/fuselage fatigue test

The subject test includes the centre and the rear part of the fuselage, the complete wing torque box and the rear part of the engine nacelles.



*Figure 14. Saab 2000, wing/fuselage fatigue test.*

The wing detail design is changed compared to the Saab 340 (machined spars with integral spar caps), and the wing/fuselage interface also. Furthermore the cabin pressurisation spectrum is more severe, more exactly twice as severe as the spectra for the Saab 340 aircraft. The flight and landing loads on the fuselage is also more severe due to the slender fuselage of Saab 2000.

The first part of Wing/Fuselage Fatigue test up to 150000 flights with fatigue loads is finalised. Subsequently, the damage tolerance testing will continue aiming to reach 2\*12000 flights with artificial notches. Twenty six different types of damages have been defined reflecting the damage tolerance characteristics of various principal structural elements of the Saab 2000 airframe.

In conformity with other tests, the wing/fuselage structure will be tested to demonstrate the damage tolerance characteristics in accordance with airworthiness requirements specified in FAR/EASA regulations. This also includes residual strength tests up to limit load condition for selected and critical load cases.

The test sequence used in the damage tolerance phase is the identical to sequence used in the fatigue phase. Thus, this sequence is truncated in terms of reduction of load cycles with small ranges. For damage tolerance testing is also crucial to consider load cycles will small amplitudes or ranges due to the contribution to the total crack propagation.

Instead of using a revised test sequence it has been verified that the existing sequence can be adapted with the addition of more test cycles to the previous defined test sequence.

Since a limited no of damages shall represent damage tolerance characteristics of all critical parts, a careful selection has been carried out.

The criteria for selecting which damages to test have been:

- Damages with impact on flight safety
- Damages with short calculated total crack growth life
- Damages in fail safe structure, for which the calculated crack growth life after failure of one load path is short
- Damages for which it is desirable to improve the in-service inspections

The selected damages cover different types of structural parts, such as wing panels, wing spars, fuselage panels, reinforced fuselage cut-outs, wing and fuselage splices. They also cover different types of crack origins, such as for example free edges, open holes and holes with pin load.

Figure 15 summarizes the location the artificial cracks introduced on the Saab 2000 airframe. Figure 16 shows an artificial crack in the forward lower spar cap including a similar damage to the outer wing skin (damage #19). Figure 17 shows an example of introduced artificial cracks on the lower wing panel (damage #16), the internal located stringer is also simulated to be broken (through cutting of the entire stringer)

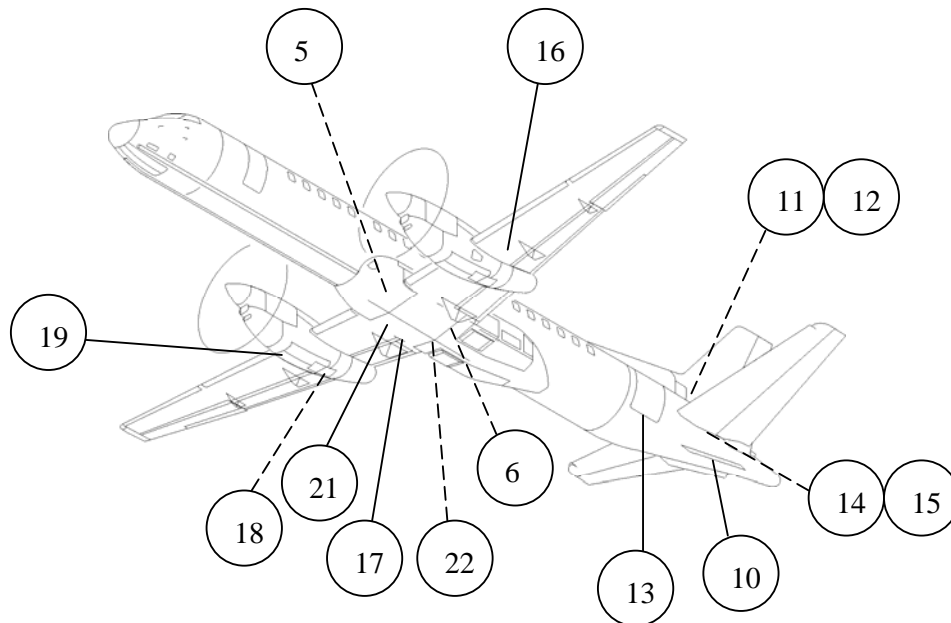


Figure 15. Saab 2000 Overview of artificial cracks in test article.

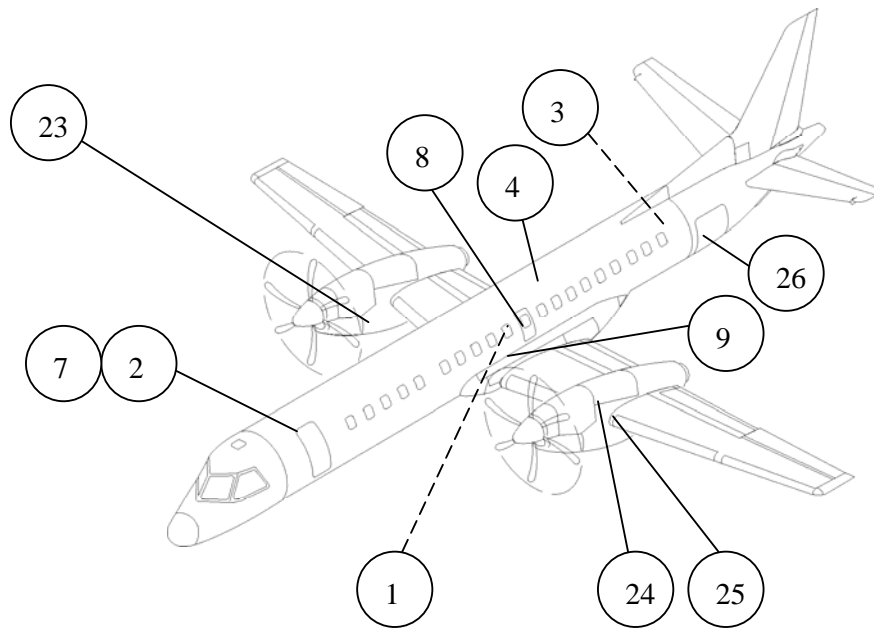


Figure 15 (cont.). Saab 2000 Overview of artificial cracks in test article.



Figure 16. Saab 2000 Artificial crack in lower forward wing spar cap and in skin

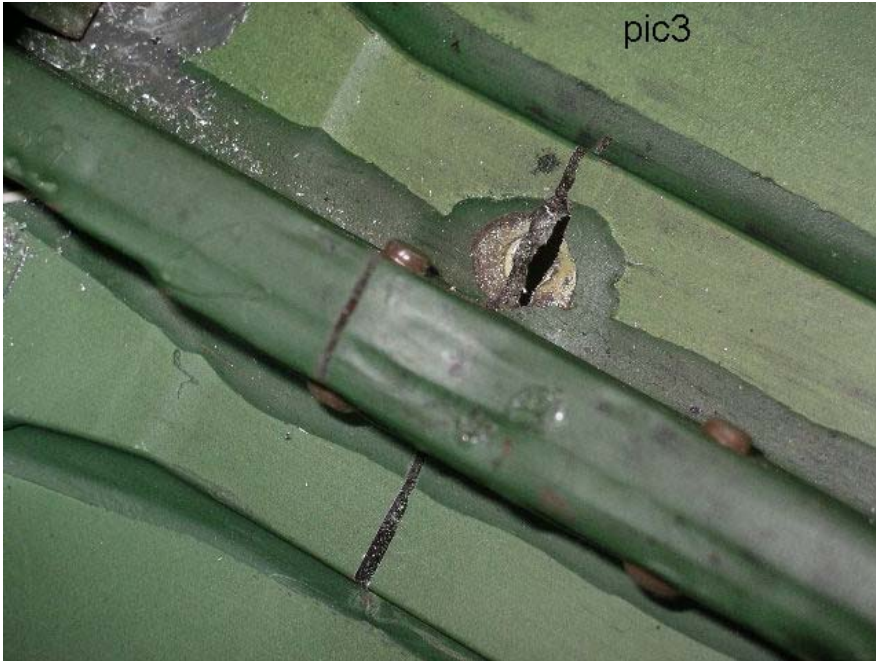


Figure 17. Saab 2000 Artificial crack in lower wing skin with a broken stringer.

In general, it is observed that it is hard to have a natural crack growth from an artificial damage. Theoretical crack growth analysis appears to be afflicted with some conservatism. Analytical damage tolerance models are mostly limited in geometry and redistribution of internal loading to adjacent members are not always considered. Consequently, analytical prediction using classical fracture mechanics is deemed to be slightly conservative compared to the results obtained from full scale damage tolerance testing. However, the artificial crack (damage 16) in the lower wing skin, figures 18 and 19, has been propagated towards the adjacent stringers and crack arrest has been noted at the bonded stringers. The initial crack was 55 mm including a broken stringer, the crack has been propagated 280 mm under 36000 flights of testing. The two-bay crack philosophy has thereby been verified for a predefined inspection interval.

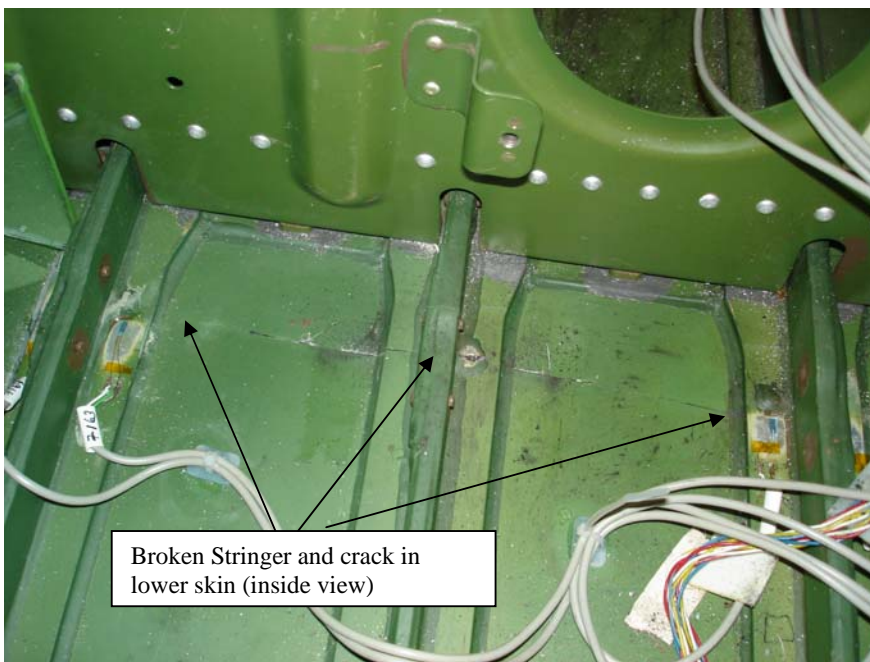


Figure 18. Saab 2000 Artificial crack in lower wing skin and stringer -inside view.

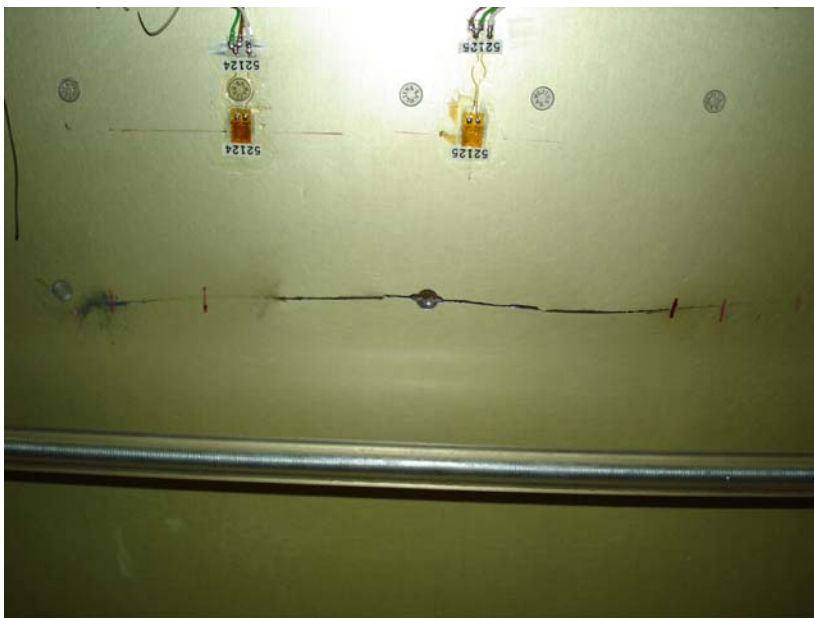


Figure 19. Saab 2000 Artificial crack in lower wing skin and stringer -outside view.

The damage tolerance testing has also revealed that welded structural elements are sensitive to fatigue and crack propagation. Experiences from fatigue/damage tolerance testing report that the structural trussgrid for attachment of the Auxiliary Power Unit was failed at a late stage of the testing. One of the strut members was discovered to be broken as outlined in figure 20. Welded designs are normally influenced by heat affected zones impairing the fatigue and damage tolerance characteristics. Adverse stress concentrations in combination with local load transfers contribute also to the failure of the welded strut.

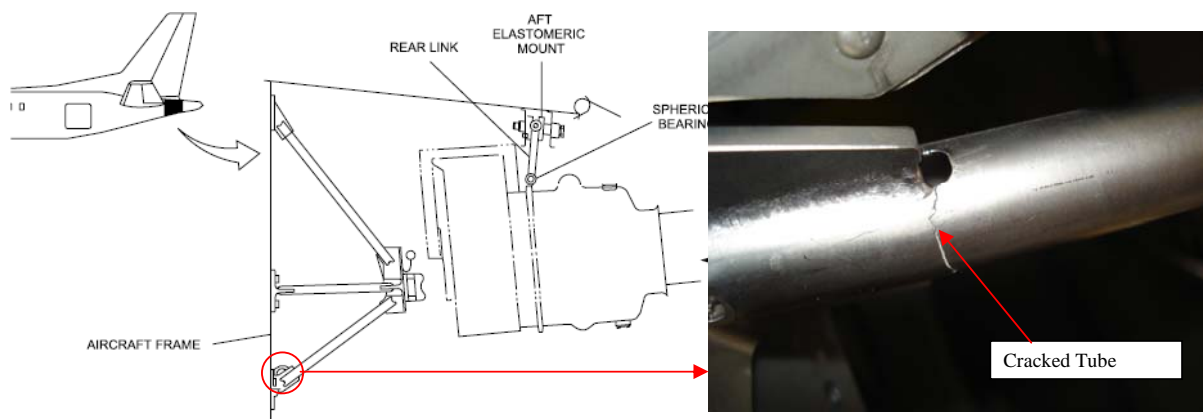


Figure 20. Saab 2000 APU attachment failed strut due to fatigue/damage tolerance

### 3.3.3 Saab 2000 Verification of structural repairs with respect to additional authority requirements

In addition to this, there is a program ongoing to enhance the continuing airworthiness with respect to structural repairs and alterations. The Aging Airplane Safety Rule (AASR program) is mandated by the European and the US Authorities, calling directives to the manufactures to address fatigue/damage tolerance issues considering structural repairs and alterations.

A set of additional rules named FAR 26 has been released in order to focus on damage tolerance characteristics on structural repairs and alterations. Fatigues cracking of aforementioned items have been a major aviation safety concern for many years. Unless detected and repaired, fatigue cracks can grow to the point of catastrophic failure. Subsequently, the incident with the B 737 in 1988 resulted in major structural failure of a primary element. Highlighted aged-related problems with airframe structural fatigue and issues regarding maintenance, inspection, and repairs were contributing factors to the incident.

This initiated comprehensive research and engineering work to minimize future and hazardous structural issues. Following the new set of retroactive requirements, the test airframe of Saab 2000 will be utilized for verification of generic structural repairs with respect to fatigue and damage tolerance characteristics.

### 3.3.4 JAS39 Gripen Fatigue Testing

The strength verification programme with large components was completed during 1994. The full scale fatigue test of the twin seater, 39B, was completed in 2000. The full scale fatigue test of the single seater, 39A, was tested much further in order to verify an extended life of the wing and fin of the C/D versions and was completed in 2007. The full scale fatigue test of a twin seater export version, 39D was completed 2008.

### 3.3.5 Continuing fatigue testing of the single seater, 39A

Details about the test and results found during testing to 32,000 flight hours can be found in the previous Swedish review [1]. During 2009 the tear-down inspection will start. Before the disassembly takes place, the test article is used for additional testing of the wing mounted weapon pylon stations. The aim of the testing is to pave-the-way for the airframe for extended flight time with external stores and for future integration of new weapons presently not known. The testing is done for pylon stations 1, 2 and 3.

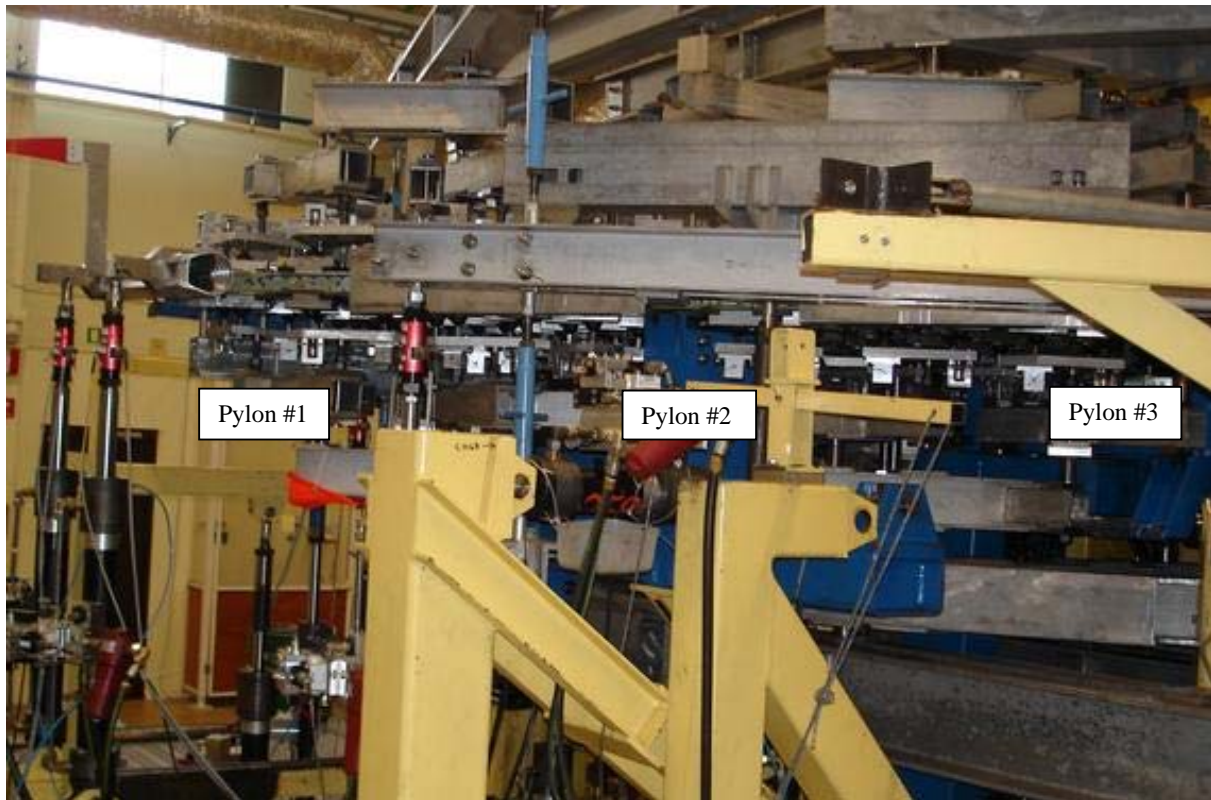


Figure 21. Continuing testing of weapon pylon stations using Gripen A full scale test article.

### 3.3.6 Full scale fatigue test of the twin seater export version, 39D

The test object is a complete fuselage, figure 22. Attachment loads from the wings, fin, foreplanes, landing gears etc. are applied via dummies. Details about the test and testing aims can be found in the previous Swedish ICAF review [1]. The fatigue testing was started in January 2004 and reached the target life 32,000 hours in December 2008.

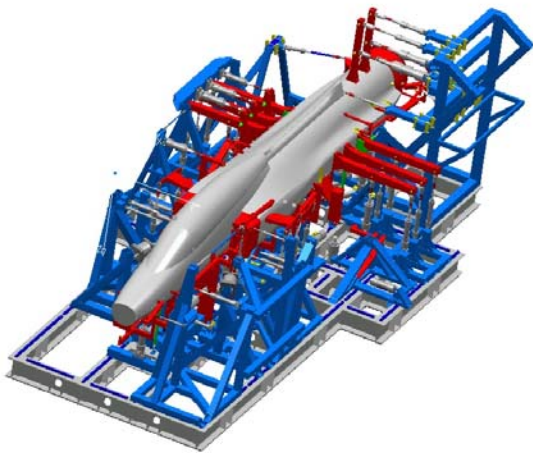


Figure 22. Gripen twin-seater 39D. Schematic drawing and a photograph of the of the forward fuselage with the air-to-air refuelling probe dummy.

Major inspections were done at 8,000, 16,000, 24,000 and 32,000 hours. No fatigue cracks have been found in primary structure. The very few cracks found have occurred in secondary structure:

- In a lug for the attachment of the actuator for the main landing gear door, figure 23.
- In a lug for the attachment of the actuator to the air-brake, figure 24.
- In a sheet strap connecting a frame to the engine wall in the rear fuselage, figure 25.

Improved replacements of cracked parts have been designed.



Figure 23. Cracked lug for the attachment of the actuator for the main landing gear door

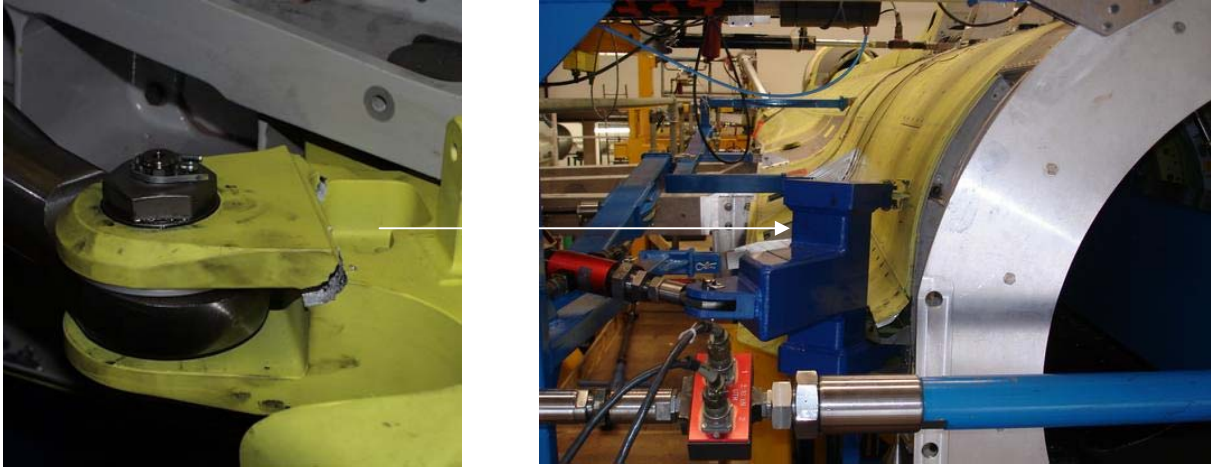


Figure 24. Cracked lug for the attachment of the actuator to the air-brake

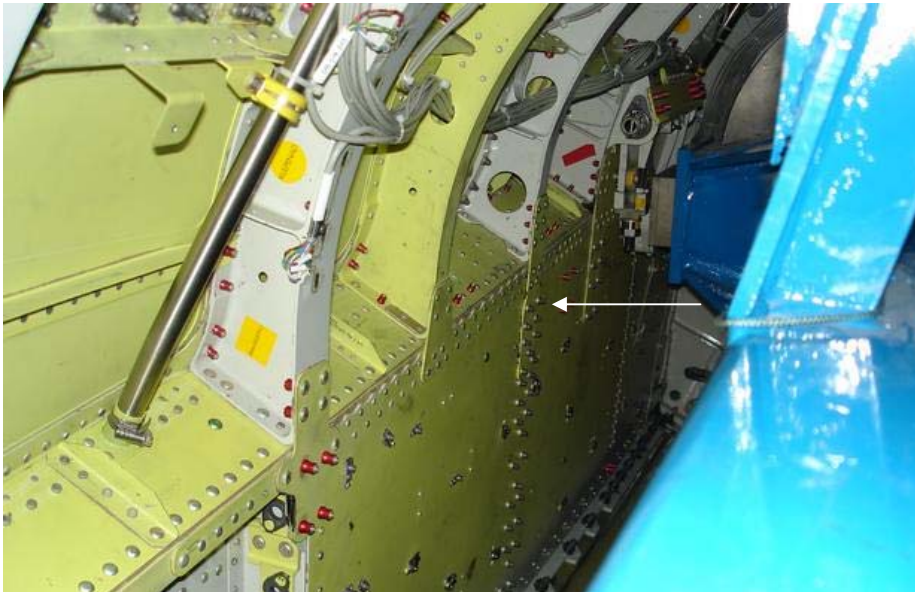


Figure 25. Cracked sheet strap connecting a frame to the engine wall in the rear fuselage.

During 2010 the tear-down inspection will start. Before the disassembly takes place, the test article is for the same purpose as for the single seater test, used for additional testing of the fuselage mounted weapon pylon stations. The testing is done for pylon stations 4 and 5. It may also be extension of the testing to verify more air-to-air refuelings.

### 3.3.7 Export Standard Pylons Fatigue Tests

The development of weapon pylons, covering both wing and fuselage mounted pylons, compatible for NATO stores for the Gripen fighter was initiated in 1997. Common to all pylons are a box structure design built around a mechanism by which the stores are pre-tensioned to the pylon.

To support static stress analysis, some static tests where performed. Static strength requirements where defined as: no permanent deformation allowed at 100 % limit load and no failure allowed at 150 % limit load.

Failure of outboard wing pylon #2, was reached at 300 % limit load, no permanent sets where observed at 100 % limit load. Analysis predicted failure at 240 - 290 % limit load (friction dependent load paths caused the scatter). The inboard wing pylon #3 was tested to 225 % limit load without failure with only minor permanent sets at this load level. The off

center fuselage mounted pylon #4, reached failure at 300 % limit load, no permanent deformations was detected at 150 % limit load.

The fatigue test rig is identical to the one used for the static tests, figure 26. The test rig set up is similar for all the pylons. The pylons are mounted up side down with a stiff solid beam acting as a dummy store. Air load on the pylon are applied using two cylinders with pads distributing the load to the sideplates. Air and inertia store loads are applied on the dummy store using seven cylinders. Pretension and release of pretension of stores are also simulated in the fatigue test by using an electric torque wrench operated by the test rig control system.

The initial aim of the fatigue test, common to all the pylons, is to verify a safe life of 4000 flight hours by 16000 flight hours of testing. By extended fatigue testing an optional safe life requirement of 8000 flh could be reached.

Every 4000 flight hours of testing is followed by NDT-inspections of critical areas, using methods such as Eddy current, Fluorescent Magnetic particle and Penetrant, where applicable. Furthermore, the pretension of the bolts in the pylon to wing joint is also checked by a Raymond Bolt Gauge test.

The Pylon #4 fatigue test reached 16000 flight hours of testing without any cracks detected, verifying a safe life of 4000 flight hours. Due to a change in material of the bolts connecting the store mechanism to the pylon, the fatigue test was extended to 48000 flight hours of testing. No cracks were detected after 48000 flight hours of testing, thus also verifying the optional safe life requirement of 8000 flh. Later on, the Pylon #4 fatigue test object was reused in the previous described static test.

The fatigue test of Pylon #2, #3 and #5 have all reached 16000 flight hours of testing without any cracks detected, verifying a safe life of 4000 flight hours. The initial aim of the fatigue test has been reached and at the moment no demand for verification of the optional safe life requirement of 8000 flh has been raised, thus no further testing is planned.

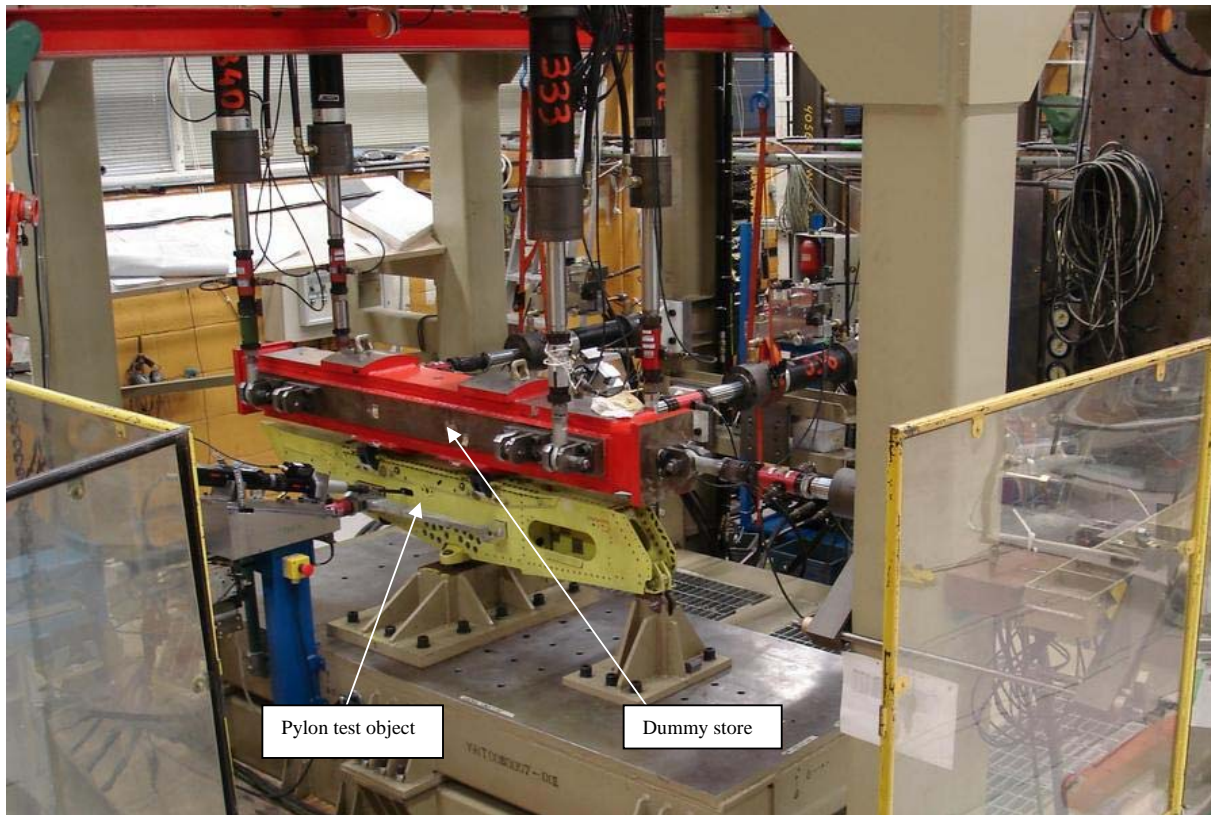


Figure 26. Export pylon static- and fatigue test rig.

### 3.3.8 Refuelling Transfer Units Fatigue Tests

Changed fatigue requirements on the aircraft refuelling equipments have been introduced on Gripen. An evaluation of historical qualification data therefore was considered necessary. For some units in the fuel system, a satisfactory result was not present in terms of verified fatigue strength. Based on equipment designs and existing qualification data package, a set of short term actions have been closed for the Forward and the Aft Refuelling Transfer Units (FRTU and ARTU):

- Load statistics from the Swedish Air-Force.
- Design load sequences for the units.
- Strain measurements and/or stress analyses on the units.
- Residual strength and/or fatigue testing of the units.
- Inspection programme on pre-flight aircraft.
- Assessment of fatigue cracks and fracture surfaces with respect to reliability in NDT-inspection (Eddy Current and Penetrant).

The following main results with respect to fatigue are defined based on performed short term actions:

- The risk for fatigue cracks on the ARTU within specified aircraft service life can not be ignored regardless of aircraft versions. The level of risk however is affected by the aircraft version. Stable fatigue crack growth and damage tolerance, has been demonstrated by fatigue and residual strength testing.
- Structural areas with limitations in fatigue strength have been identified by stress analyses, fatigue testing and inspection programmes. Test rig results harmonize with in-service experiences.
- A Technical Sheet on local and focused NDT-inspection has been specified for the ARTU. Significant mechanical residual stresses in compression are present at the reinforcement ribs run-outs.

Decision was taken to upgrade the refuelling transfer units. In the case of the ARTU, the modifications concerned both valve closure/indications and mechanical strength properties. The mechanical strength would be improved by redesign of the manifold body and stronger screws between the manifold and main body. The redesign process began by establish an FE-model of the original manifold design.

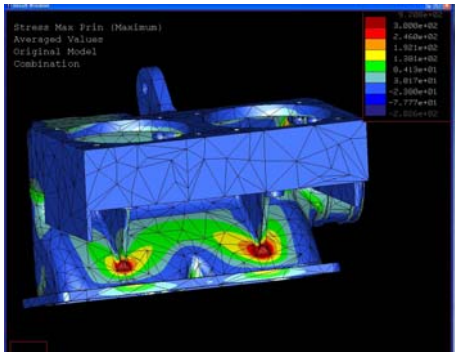


Figure 27. FE-model of original manifold design.

The high stressed areas were identified and reinforcement work proceeded but within certain limitations:

- Interface points with aircraft structure must remain unchanged to avoid costly redesign and modification of the current pipes.
- Keep weight increase to a minimum.
- Fuel flow must remain unchanged (i.e. only small changes in the interior volume of the manifold is allowed)

Based on results from FE-analysis, design changes were proposed:

- increase of the thickness from 2 to 3.5 mm (yellow color)
- changed contour of the two stiffness ribs and thickness increased from 3 to 6 mm (red color)
- radius 3 between stiffness ribs and casting surface (red color)
- radius 3 around the mounting flange, except at the six holes where the washers need to be put (radius 0.5 mm) (orange color)

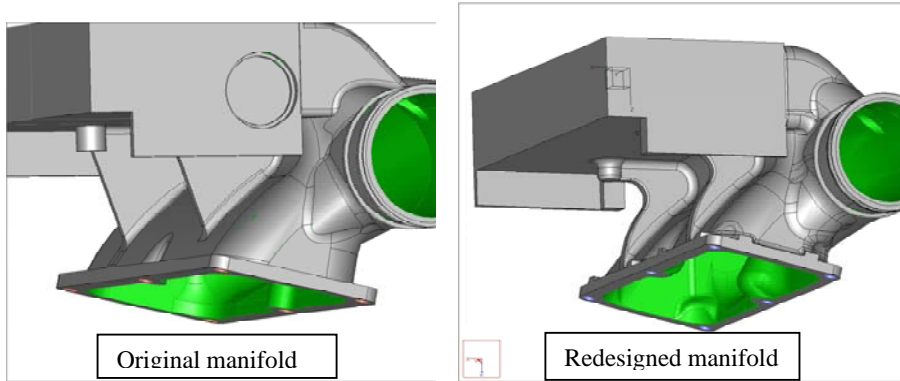


Figure 28. 3D-view of original and redesigned manifold.

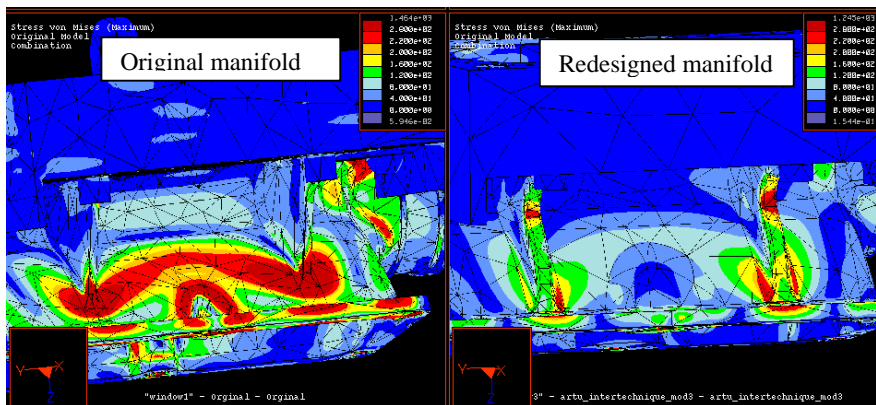


Figure 29. stress plot of the area around the stiffness ribs.

Fatigue analysis based on results from the FE-model were carried out on the redesigned manifold and sufficient margins of safety were achieved. Fatigue test on the redesigned manifold were carried out at Saab. The loading was a pressure sequence and the number of load cycles corresponded to twice the required safe life (i.e. 8 times the service life).

- Before the test start strain gauges were applied and strains for a static pressure were measured and compared with results from the FE-analysis. The measured strains were found to be similar with the analysis results.
- Inspections were carried out during and after test. Penetrant and eddy current methods were used.
- The results from the fatigue test were satisfactory. No indications from the inspections were found.

Static test to levels above ultimate load on the redesigned manifold were also carried using the test specimen from the fatigue test. No permanent set or leakage were found, test stopped due to a broken seal.

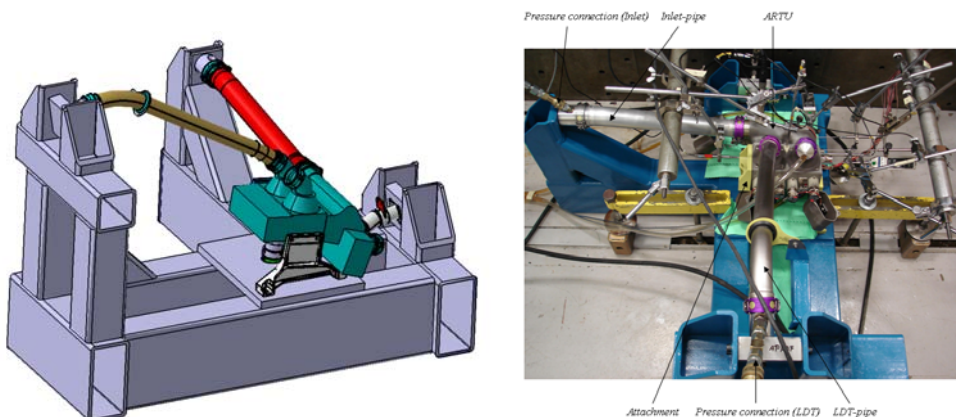


Figure 30. Test set-up

### 3.4 FATIGUE CRACK INITIATION AND PROPAGATION

#### 3.4.1 A Case Study of Multiple-Site Fatigue Crack Growth in the F-18 Hornet Bulkhead

The numerical results given here are obtained by FOI within the framework of the Finish-Swedish cooperation (VTT, Patria Aviation and FOI) contracted by the Finish Air Force. Further information is found in [3] and in the Finish ICAF review [4].

A novel methodology for fast and accurate calculations of stress intensity factors for multiple-site crack scenarios has been derived. This methodology makes it possible to study multiple-site cracking and also statistical modelling of crack growth in detail, as millions of stress intensity factors can be computed virtually exactly, in short time on parallel computers.

The fracture mechanics modelling has been used to predict cracking in an I-beam type of specimens representing the FINAF F18 Hornet bulkhead, see Figure 30. For this purpose, fatigue crack predictions have so far only been done without considering any crack retardation phenomena due to load interaction effects under spectrum loading. Such features may be included in the future. When accounting for the 5% difference in local strain levels that were observed when comparing accurate stress analysis of the un-cracked structure to actual strain measurements, predicted crack growth behaviour agreed well with experimental observations. Further validation of the derived methodology will be possible after new experiments with marker loads facilitate back tracking of the crack morphology down to small crack sizes.

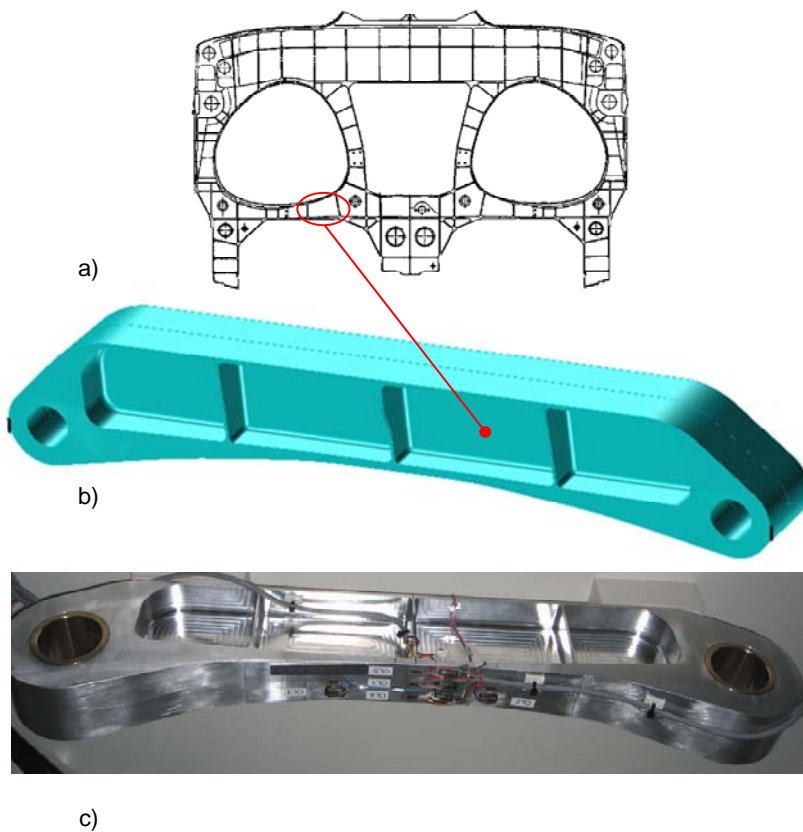


Figure 30. – Geometry of studied test object. Picture courtesy of Patria Aviation (b, c).

a) Schematic geometry of the bulkhead Y488 of the F/A-18 Hornet [4],

b) An isometric view of the I-beam specimen simulating a detail of the bulkhead, c) An example of one I-beam specimen equipped with strain gauges.

Modelling including the interaction of multi-site cracks showed that the interaction effects only take place rather late in the overall life. This effect, however, depends on geometry, load level, and crack patterns, and may be quite different in other situations. The etching pits, in the order of 0.1 mm, were found to shorten the fatigue life substantially, by removing the crack initiation phase.

A statistical analysis that considers three initial flaws located at the observed experimental initiation points, see Figure 31, showed how such analyses can be used to improve the understanding of early crack growth behaviour. By assuming that the three initial flaw sizes are randomly distributed from one tenth of the crack length used in the previous discrete predictions, up to that very length, i.e. 0.127 mm, failure will occur after roughly the same overall number of loading blocks as for the discrete analyses. The variation in life from a 10% failure probability up to a 90% failure probability is around a factor of two, see Figure 32.

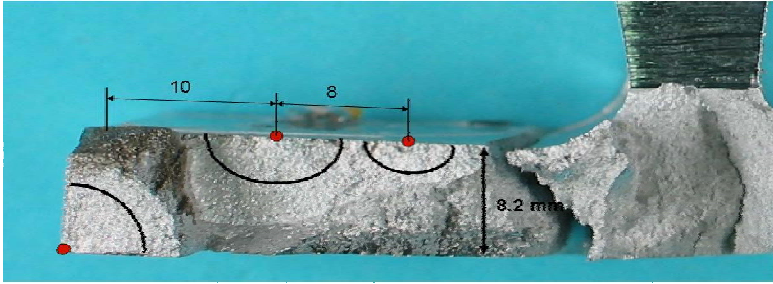


Figure 31. Fracture surface of test specimen no. 3 showing at least three nucleation sites.

The performed analyses constitute the first application of the new methodology. In the future such modeling may certainly be taken further on the present bulkhead structure, in conjunction with more detailed fractographic work on the behaviour of early crack growth. Another obvious application of the methodology derived here is the aging aircraft problem. For all aging aircraft fleets, the present procedure may assist in taking well informed decisions on life extension programs, inspection intervals, or removing the aircraft from service.

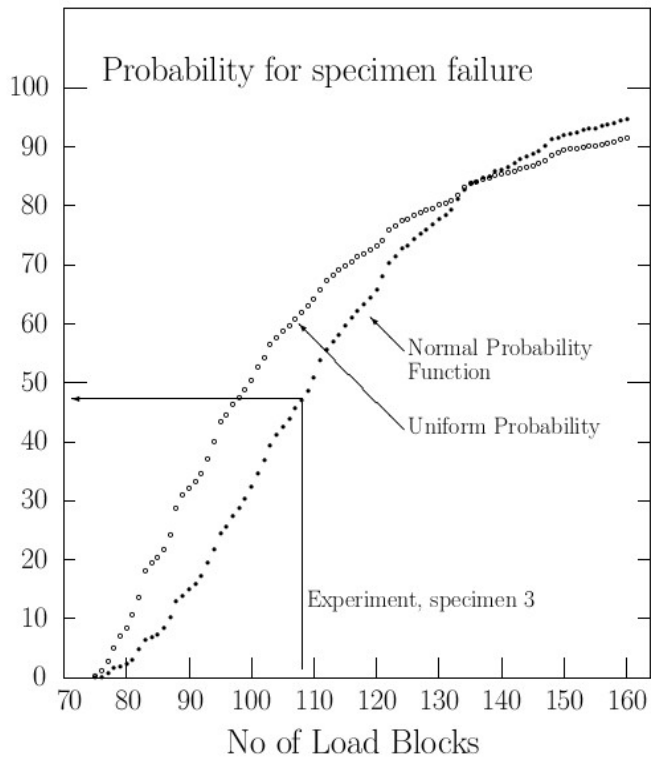


Figure 32. Calculated distribution functions showing the number of load blocks until failure for two initial crack size distributions at the three crack locations in specimen 3.

### 3.4.2 Crack growth simulation for stiffened panels [5]

Within EU 6 frame DaToN STREP proposal, it has been decided to investigate in more depth the problem of a fatigue crack running towards an integral stiffener and to assess the capability of the stiffener itself of slowing down the fatigue crack growth and of acting as an efficient crack stopper. For this purpose, a test panel with two stringers has been defined, with two blade stringers, spaced apart at 150 mm. The global dimensions of the panel are 450 mm in width and, for a proper load introduction (and a well designed aspect ratio), 1000 mm in length.

The test activity is subdivided among various partners, following their availability and interests. Since DaToN is an analyzing intensive project, an analysis of the test object will give a good reference to guide both fatigue crack growth tests and the residual strength tests. In these analyses, the linear elastic FEA computation has been made. The maximum stress is 100 MPa on the skin at the center of the panel. The FEAs are performed based on Young's modulus for the panel with or without crack. A crack with the size reaching to the root of stringer is considered.

The comparison between measured strain and the computed strain from FEA at 100 MPa is shown in Figure 33. Generally, there is a good agreement between the measured and FEA results except the data at the top of stringers. Since there is a strong indication of buckling at the top of stringers as the results in the figure shows, the measured results will be lower than that of the FEA results since the small displacement assumption has been used for the linear FEA analyses. More advanced FEA solution seems to be needed for further evaluations.

## Comparison with FEA results

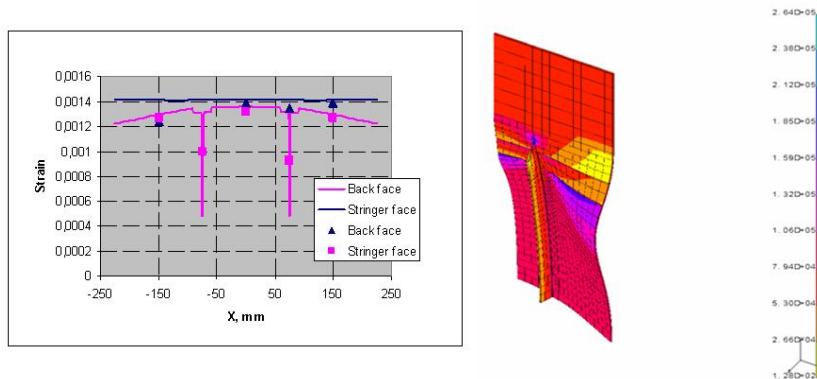


Figure 33. Comparison of FEA results and strain gauge measurements.

Five stiffened panel have tested at FOI for 2024-T3 material. The test panels are produced with high speed cutting (HSC) technique. Three of the tests are performed according to the common test program and two are extended tests.

For the common fatigue test program for the constant amplitude loading condition, one panel is tested with a stress ratio of  $R=0.1$  and maximum nominal stress of 80 MPa and another is with a stress ratio of  $R=0.5$  and the maximum nominal stress about 110 MPa. The fatigue crack propagation is recorded from initial crack until the failure on both side and faces of the panel.

One residual strength test is performed for a total initial crack size of 180 mm created by the fatigue loading. The crack growth under slow and displacement controlled mode is monitored and recorded.

In addition, two extended fatigue tests are designed and performed for the same fatigue loading conditions as those of the common test program, but with the test panels strengthened with composite strips near the stringers, see figure 34. The fatigue crack growth is recorded. The tests do not shown any improvement of the composite strips in retarding

fatigue crack growth. It does show that the bonding between the composite strips and the panel holds until failure. The placement of the strips together with undersize in cross section are considered to be the main reasons. All the crack growth tests show similar crack growth behavior as the results in figure 35 shows.

## Glass fiber enforced

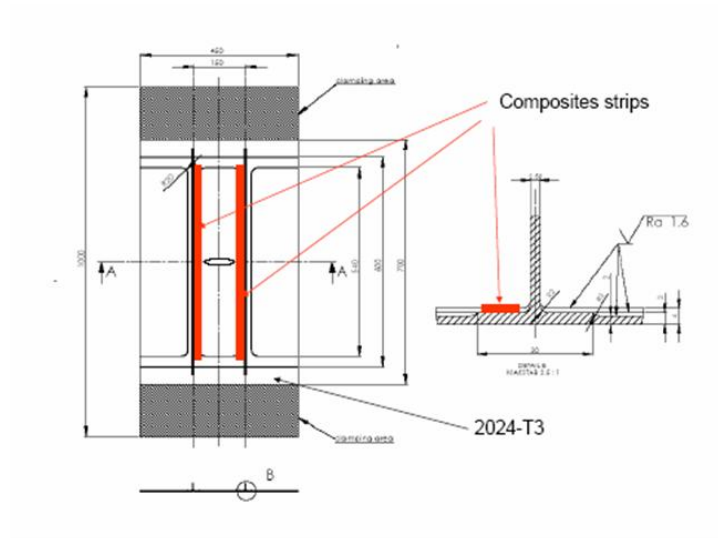


Figure 34. Schematic of reinforced stringer with glassfiber strips

## Fatigue Test Results, $a_0=10$ mm

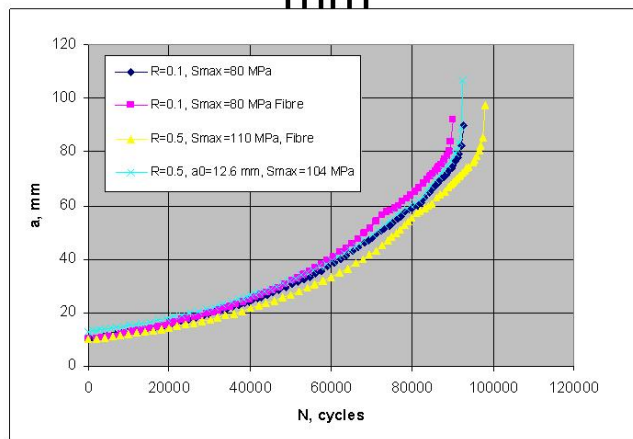


Figure 35. Comparison of fatigue crack growth results for DATON panel tests.

### 3.4.3 Validation of Damage Tolerance Analytical Models [6]

Within DaToN project, the fatigue crack propagating stopping capability of stringers in stiffened panels and their residual strength are a major concern. WP 4 is planned to validate all the methodology developed within the project to reveal issues when using these methods. The in-house developed elastic h-p finite element code STRIPE, and the strip yield fatigue crack growth simulation code CLOTEST, at FOI, the Swedish Defence Research Agency, are extended for the DaToN project to deal with damage tolerance issues of the integral structures.

Three objects are to be used for the validation purpose: one two stringer panel designed for the DaToN project, one five stringer panel used in one partner before (NLR), and one seven stringer panel tested at Airbus facility.

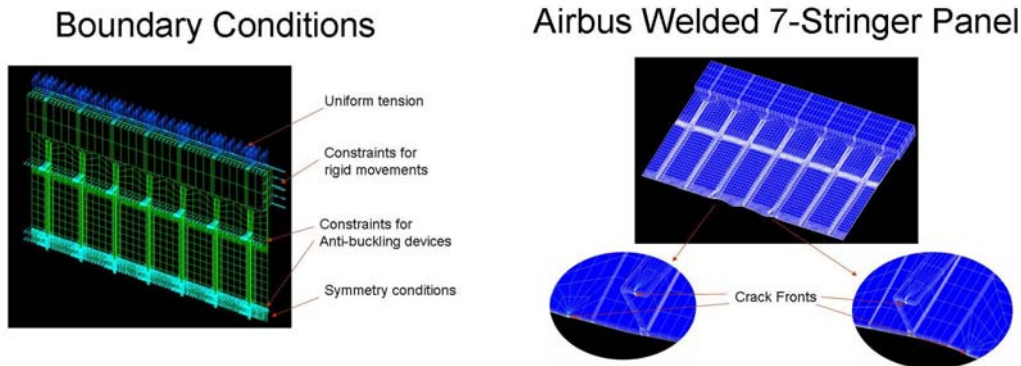


Figure 36. Finite element model and the boundary conditions for one stiffened panel.

The SIFs were firstly computed based on the assumption of linear elastic small deformation solution using such model as shown in figure 36. Some of the computed results are shown in a comparison in figure 37. Two maximum load cases are considered; one for the test with stress ratio of  $R=0.1$ . For this stress ratio, the maximum stress level is 80 Mpa for the nominal stress at the crack section. Another results are for a higher stress ratio tests ( $R=0.5$ ). For this case, the maximum stress level is 110 Mpa.

The computations showed excessive out of the plane displacement, indicating that at least the geometrical nonlinearity should be considered. Further computations were performed with the model of geometrical nonlinearity. The SIFs from the nonlinear computation are compared in figure 37 for both the 80 Mpa and 110 Mpa load level. The nonlinear results are significantly lower than those from the linear computations for both 80 and 110 Mpa stress level.

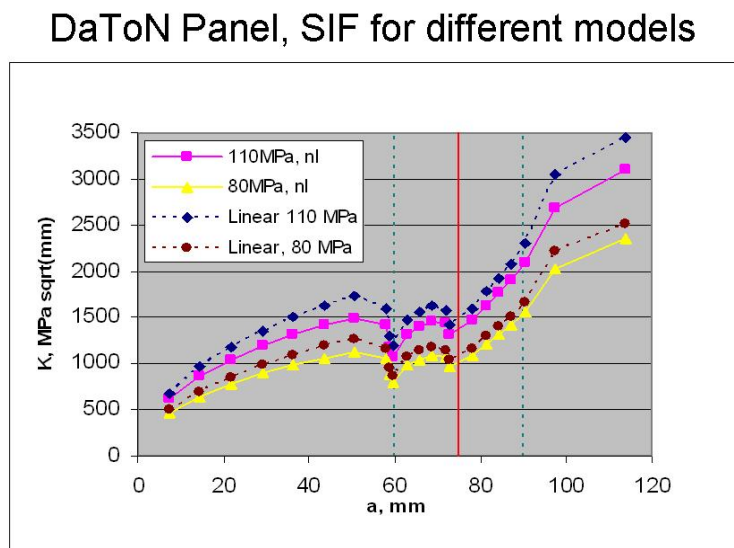


Figure 37. Comparison of SIFs for DaToN panel

The errors are shown in figure 38 when SIFs from linear computations are compared to SIFs from the nonlinear computations. The error increases with the increase in the load level. They are low for the small crack size and when the crack crosses the stringer, but still shows at least larger than 6% even for the load of 80 Mpa.

When the load increased to 110 Mpa, a maximum error as large as 16% appeared when the crack approaches to the edge of the pocket. Even for the load of 80 Mpa, the error is still 12%. This example shows that when the solid elements are used to model the sheet structure, it is necessary to use a correct model. The small deformation linear elastic model is no longer useful for such a model. Non-linear model is needed even when the material is still in the small elastic deformation regime. The excessive geometrical deformation due to the slim construction will violate the small deformation solution which usually works well for the solid structural problems.

DaToN panel: errors in linear assumption

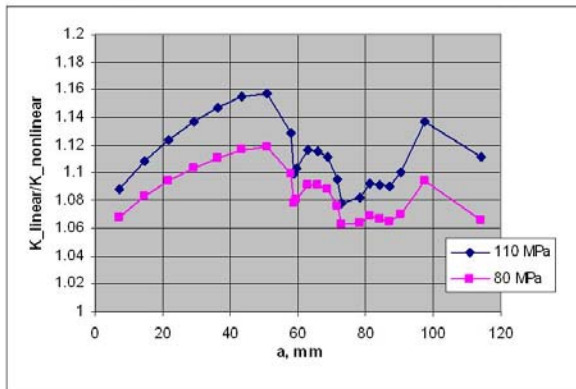


Figure 38. Errors of linear assumption

To understand the damage tolerance behavior of the integral structure made of production methods like various welding techniques, one of the important aspects, the residual stress, should be considered as well. It is well-known that any welding or cutting technique will introduce residual stresses in the structure due to the localized heat input and large plastic deformation. The difference in temperature during the cooling process as well as localized permanent deformation will introduce significant residual stresses. One obvious residual stress effect is the distortion of structure. Another less obvious effect is the strong residual stress induced by the process.

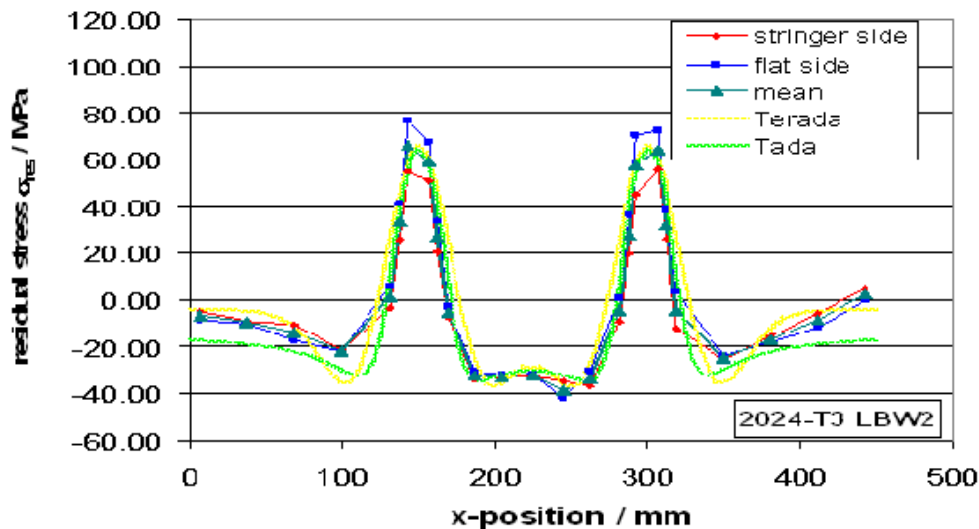


Figure 39. Example of residual stress distribution for a welded DATON panel

Some of the partners have performed the measurement with a series of strain gauges placed along the crack line. These strain gauges will reveal the distribution of residual stress when the panels are cut into the half along the crack line for

all the manufacturing techniques and different materials. Figure 39 shows one of the measured residual stress distributions for DaToN panel in a laser beam welding condition.

To account for the residual stress effect, a strip yield model is considered. This model is based on the Dugdale assumption of the crack tip plasticity according to the elastic-plastic fracture mechanics theory. The plastic deformation, or the plastic stretches, is considered during the whole fatigue crack growth process. The advantage of using the strip yield model is that the requirement for the experimental data is significantly reduced. Figures 40 and 41 shows some of the predictions from the strip-yield crack growth model when effects of welding are considered.

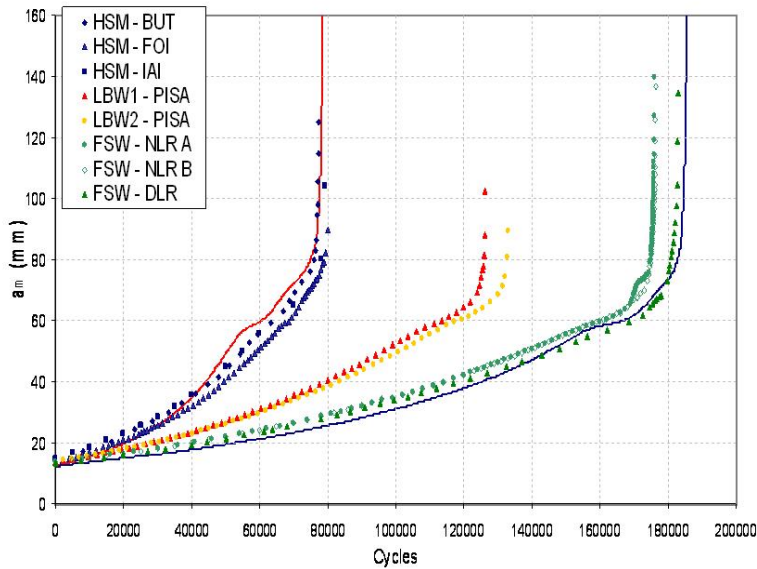


Figure 40. Comparison of prediction and test data for  $R=0.1$  and  $S_{max}=80$  MPa

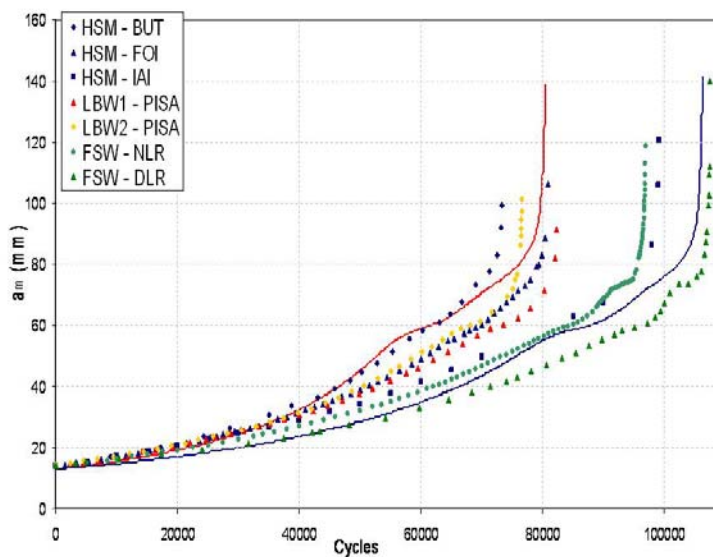


Figure 41. Comparison of prediction and test data for  $R=0.5$  and  $S_{max}=110$  MPa for reduced residual stress to 65% of original value.

The methodology for fatigue crack growth and residual strength prediction has been validated within DaToN project. There appears to be a close relation between the prediction and the test results. It shows that some aspects must be dealt with much more care so that prediction may provide useful reference. It shows that non-linear analysis is necessary in FEA when the solid model is used for the stiffened panel. There is a great deal to do with the boundary conditions in the numerical data. Residual stresses play a significant role in the crack growth propagation, and they could both increase or decrease the fatigue crack growth rate for the same manufacturing technique, depending on how the crack may be formed. The residual strength depends on several mechanisms and all the mechanisms should be considered.

#### 3.4.4 Stress Intensity Factors for Multiple Surface Cracks [7]

Simulation of the interaction of multiple surface cracks is one of the concerns for the structural life expectancy analyses. This paper aimed to investigate the stress intensity factors of multiple cracks which may occur due to the high stress concentration or the existence of multiple initial defects.

This project aimed to study interaction of the multiple cracks in welded locations. The study is performed with the use of a FE code developed by FOI called STRIPE. Due to several problems in the computing of SIFs with STRIPE, all objectives were not carried out.

Firstly, to quickly create a multiple cracks model a meshing code was written with Matlab. This code allows the user to create a personalized model with up to 9 cracks and to write a STRIPE input file. Secondly, the problem of direct SIFs computation by STRIPE was overcome by using the crack tip displacement field. The displacements are extracted from the output file and the SIFs are calculated using a Matlab code.

From the finite element analyses, it is found the periodic placed cracks begin to affect each other when the side-to-side distance becomes less than twice the crack surface size ( $w=6$  in figure 42), and the effect is mostly strong on the surface.

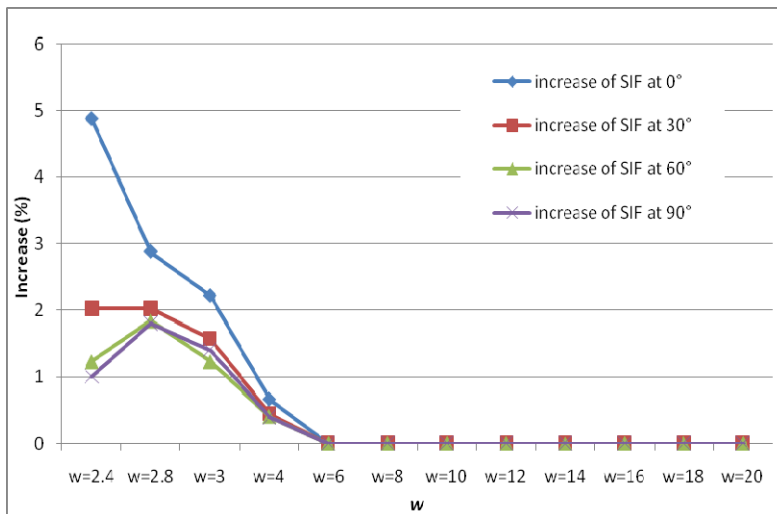


Figure 42. Interaction of periodic cracks

In order to study the interaction between multiple cracks, three 3-cracks models were created (see figure 43) with different crack sizes but sharing the same second crack and the same distance between the cracks' fronts at the open surface in order to compare the SIFs along the crack #2 edge. It is shown that the bigger the side cracks are, the greater the SIFs are, which was expected. It is also shown that the effects of the crack are seen all along the nearby crack front, not only on the side in the front.

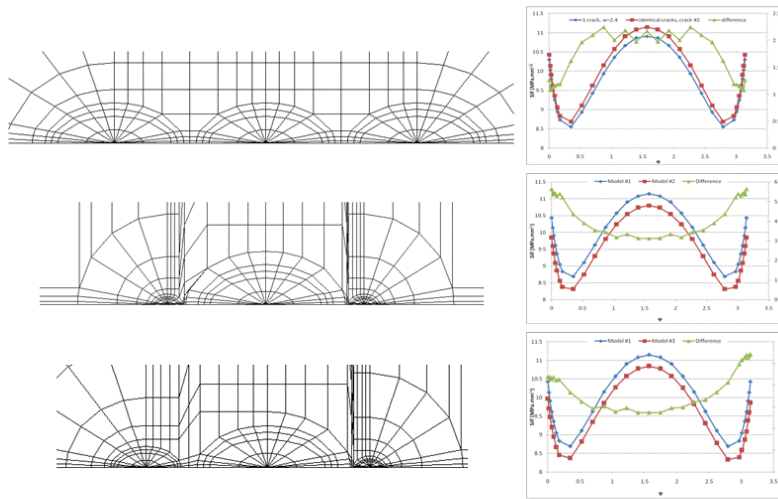


Figure 43. Interaction of irregular cracks

A more general case is considered for 9 cracks with random sizes and placements. The cracks' sizes and positions are summarised in the following table and figure 43 presents the resulting meshing. The overall computation took 5960.7 CPU seconds.

Crack	Position x	$a$	$c$
1	0.861277	0.269063	0.134532
2	4.162210	0.412069	0.206034
3	5.094520	0.246900	0.123450
4	6.580351	0.254007	0.127003
5	7.514683	0.201117	0.100558
6	9.353273	0.226393	0.113197
7	10.898561	0.279061	0.139530
8	11.902281	0.307761	0.153880
9	13.590469	1.001706	0.500853

The computed SIFs are presented side by side on figure 44, positioned on the horizontal axis according to the cracks' number. The randomization aimed to create a model with various situations with cracks close to each other's and some are bigger than the others. The SIF results suggest a highly random nature of crack initiation and propagation pattern when multiple cracks are considered.

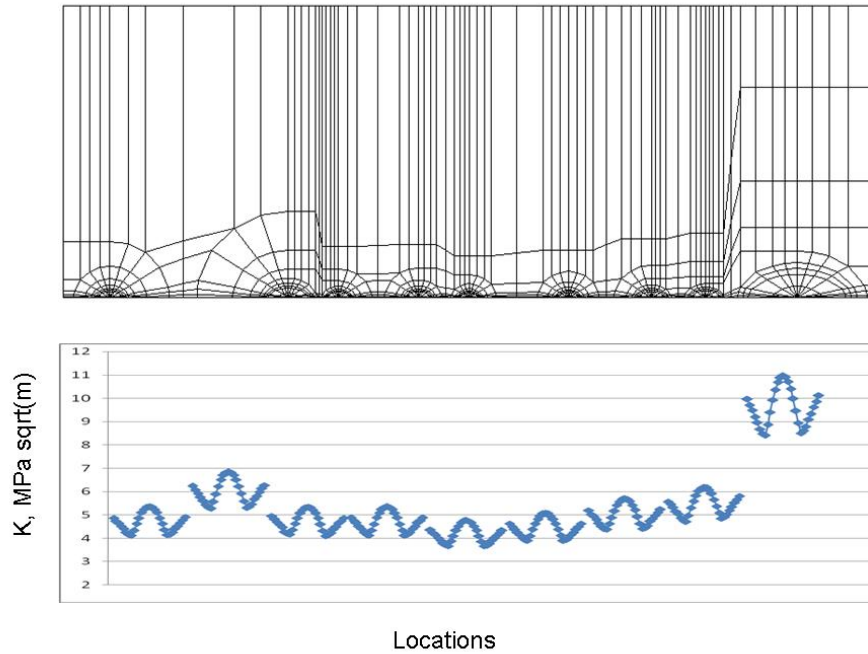


Figure 44. Interaction of irregular arbitrary cracks (9 cracks in the model)

### 3.4.5 Decreasing fatigue properties of thick aluminum plate

Decreasing fatigue properties of aluminum plate (7010-T7451 and 7050-T7451) with increasing thickness are well known. Efforts to quantify the actual levels of fatigue data have been made at Saab along with increasing use in course of time of larger plate thicknesses. In figure 45, S/N-data from constant amplitude tests (R 0.1) for different 150 mm plates are very similar and much below the old baseline for 80 mm plate. Ongoing tests of 175 mm plate indicate even lower fatigue data. Detailed knowledge of fatigue properties vs. plate thickness makes optimal fatigue design possible.

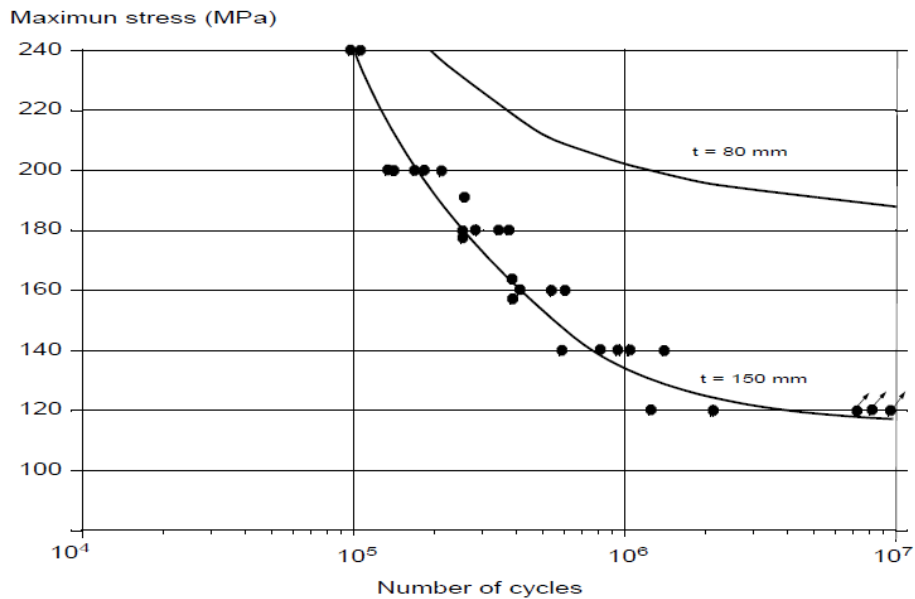


Figure 45. S/N-data from constant amplitude tests (R 0.1) for different 150 mm plates

### **3.4.6 Residual life prediction based on inspections [8]**

In laboratory studies the stress strain cycles and other similar parameters are often considered known. In real world applications this is not always the case. Still we want to predict remaining lives of the components.

In a case study the crack growth of the low pressure turbine nozzle is studied. The historical data we have is limited and we do not know the exact nature of the crack growth. The temperature cycles in the engine result in the nozzle experiencing fatigue and ultimately cracking. A nozzle is considered broken when the largest crack is above a certain level described in a set of fitness rules. The crack length is measured regularly at inspections but the measurements themselves are not used but it is only noted if the nozzle complies with the fitness rules or not.

In our study, we modeled the crack growth and managed to improve the prediction of the residual life considerably using the measured crack lengths. The estimated distribution of the residual life was updated after each inspection and the statistical uncertainties were taken into account. Since the data was very limited a very simple crack law was used, depending on one growth exponent parameter and two random variables describing the initiation time and the slope of the growth curve. The residual life distribution could then be used in a model for an optimal replacement policy of the nozzle.

## 3.5 COMPOSITE MATERIALS

### 3.5.1 Effects of CFRP laminate thickness on the bending after impact strength

More and more composite materials are used within primary load carrying aircraft structures. Examples are Boeing 787 and Airbus A350XWB where the composite content has increased to 50-60% by weight. As a reference the structural weight of the Saab Gripen fighter is approximately 25% by weight.

Due to the aim to decrease manufacturing cost the structures have a higher degree of integration and complexity. More integrated structures give fewer articles and fewer steps in the manufacturing chain. In many cases new innovative design solutions are a requirement to enable integrated structures. Good examples of this are Saab Aerostructures redesign of the A320 aileron (see figure 46) and Boeing 787 "Bulk Cargo Door", where manufacturing cost has been reduced considerably partly due to this kind of innovative design solutions.

As a consequence of this development there are more interlaminar loads (bending, transverse shear etc) within composite structures. Example of this is stringer stiffened panels (where the fasteners are substituted by matrix plastic as load carrier between skin and stringers), beam radii, areas with thickness variations, fuel pressure loads etc. Furthermore there is a strive to permit operation in the post-buckled regime, which also contributes to the out of plane loads.

Impact frequently causes damage on composite structures that may cause significant reduction in strength. Low velocity impact damage due to e.g. dropped tools, runway debris during fabrication or maintenance operations may cause so called "barely visible impact damage", BVID. This type of damage is often not visible to the naked eye and has to be observed by e.g. ultrasonic C-scan. Since there is a potential risk of undetected damage (BVID) in an aircraft structure these types of damage must be taken into consideration during design.

Traditionally the structures are designed to minimize out of plane loading, due to the composite material's low interlaminar strength. Because of this there is a lack of design tools and data that handles these loads. At Saab there exist for example extensive test results and a tool regarding residual strength of in-plane loaded composite structure. To increase the potential and reduce conservatism during design there is a need to increase the knowledge regarding residual strength of out of plane loaded impact damaged composite structure. The study presented in this work is one step towards this. Here two laminate thicknesses are tested in bending, both exposed to the same impact threat. Accompanying tests in compression are performed and reported to allow evaluation of the full effects of bending.

Saab Aerostructures manufactured laminates from HTA/6376C carbon fibre/epoxy pre-preg 5769-01. Two laminate thicknesses were manufactured, 4.16 mm and 8.32 mm, respectively. The plates were cut into specimens with a width of 156 mm and length of 260 mm and 450 mm for compression and bending tests respectively, according to the Saab internal standard. The specimens were clamped (150x230 mm) and impacted in a drop-weight rig at 35 J using a spherical tup with a radius of 12.5 mm.

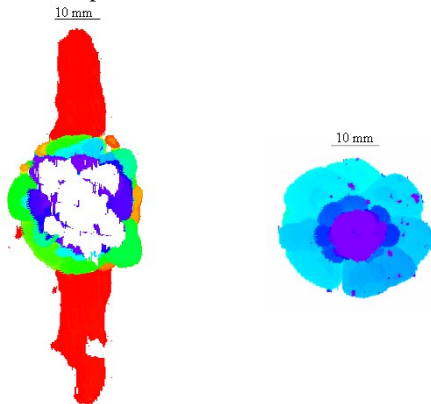


Figure 46. Damage caused by a 35 J impact on a) 4 mm (left) and b) 8 mm (right) thick laminate

As seen in the C-scan pictures in Fig. 1, the impact damage is distributed through the whole thickness in the 4 mm specimen whereas damage in the 8 mm specimen only is observed in the upper part of the specimen, as a result of high contact stresses present during impact of the thicker laminate. A fractography picture of the same damage as in figure 46 a is presented in figure 47.

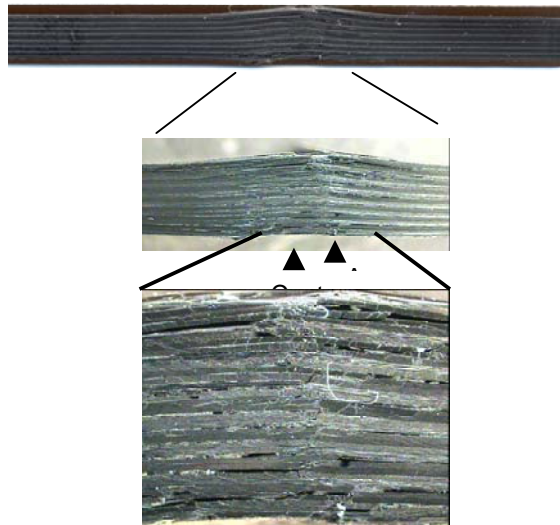


Figure 47. Damage caused by a 35 J impact on a 4 mm thick laminate

Bending tests were performed in a Zwick 150 kN electromechanical testing rig using a specially manufactured bending rig according to figure 48. The impacted side was placed on the compression and tension sides in different tests.

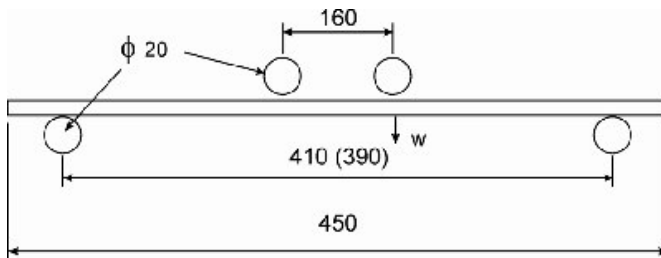


Figure 48. Bending tests of laminate with impact damage. Due to large deformations the span of the 4 mm laminates had to be reduced to 390 mm.

Compressive tests were performed on specimens with impact damage. The specimens had a width of 156 mm to fit in a rig earlier used at FOI (Swedish Defence Research Agency). Antibuckling devices were used during the tests.

As expected, the impact damage were more extensive in the thin laminates than in the thick laminates. The damage in the thin laminates was also distributed through the whole thickness, whereas the damage in the thick laminate only could be detected in the upper third of the laminate. Results from bending and compression test after impact are summarized in the table below (Failure strain is normalised with the results for the 4 mm plate loaded in compression).. As expected the far field strain at failure is considerable higher at bending compared to in-plane compression loading. Another observation is that there is lower strength when the side with the larger damage is loaded in compression. At strength calculation at design of a structure with a laminate loaded in a combination of in-plane and out of plane loads (bending) there is a potential with a stress methodology that can handle the difference in failure strain, i.e. make use of the higher failure strain in bending. The tests presented in this work are an initial step to increase the knowledge needed to determine such a tool.

		Loaded in bending	Loaded in compression
Impact energy	Plate thickness	Normalised far field failure strain	Normalised far field failure strain
		<b>Impacted side loaded in compression</b>	
35	4.16	2.00	1.00
35	8.32	2.64	2.14
		<b>Impacted side loaded in tension</b>	
35	4.16	1.84	-
35	8.32	3.08	-

### 3.5.2 Fatigue Test for Impact Damage Growth Threshold in Composite Laminates under Variable Amplitude Loading Conditions

Fatigue tests have been performed to determine the impact damage growth threshold of composites panels under a symmetrical spectrum loading condition, see figure 49. For the given spectrum the tests show that for the maximum strain less than 0.25%, there is no sign of damage development for 4 lifetimes of fatigue loading according to the C-scan inspections of the test items before and after the fatigue loading for an impact damage introduced with 35J impact energy and a 15 mm impactor diameter.

The 35J impact introduced a damage area (delamination) in the middle of thickness with an average size of 748 square millimeters. This damage location is the site of final failure in the fatigue tests when failure does occur, see figure 50.

Even though the fatigue life may be adequate for a safety factor of 4 under the increased maximum strain of 0.30%, the increase in the damage size at the end of test may introduce uncertainty in the structural integrity.

At 0.25 % maximum strain loading condition, no damage development is observed at least for 4 lifetimes of fatigue load for the given spectrum. Coincidentally, this is in a close agreement with the upper strain for the average damage size predicted based on the calculation of  $\Delta G_{th}$  with a value of 0.125 N/mm, for the initial damage size due to 35J impact energy, figure 51.

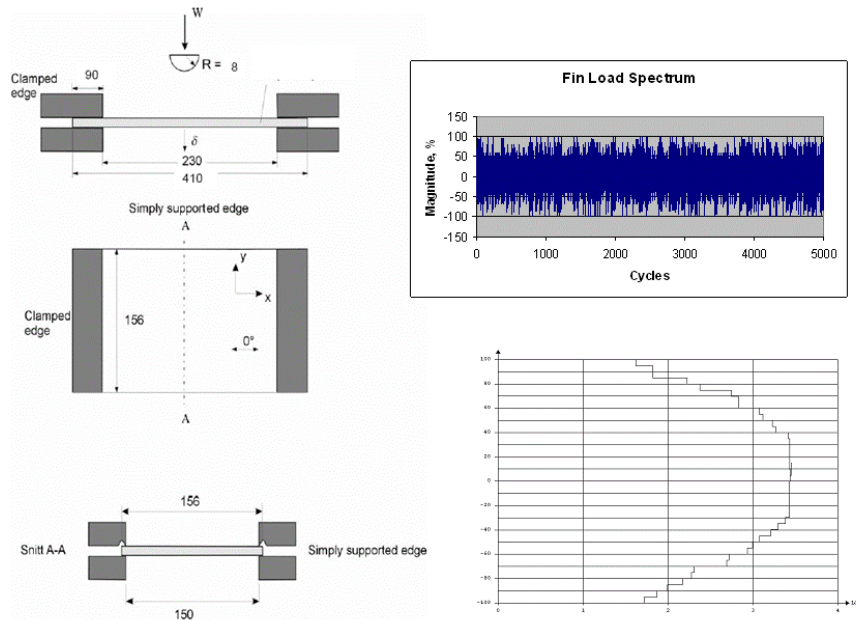


Figure 49. Impact damage and fatigue loading for composites laminates.

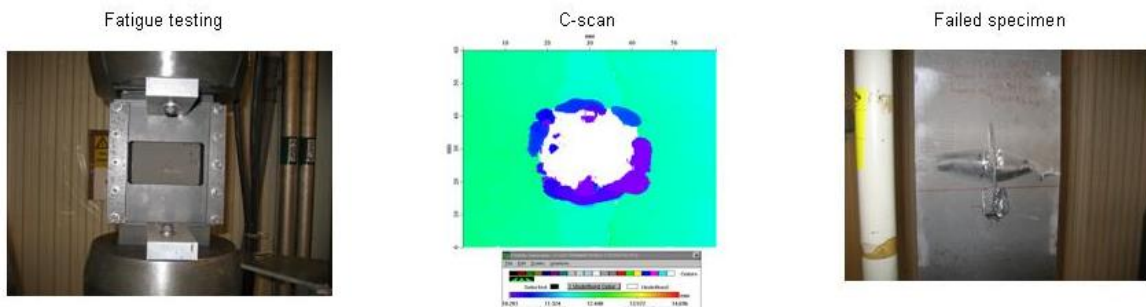


Figure 50. Test set-up and specimen

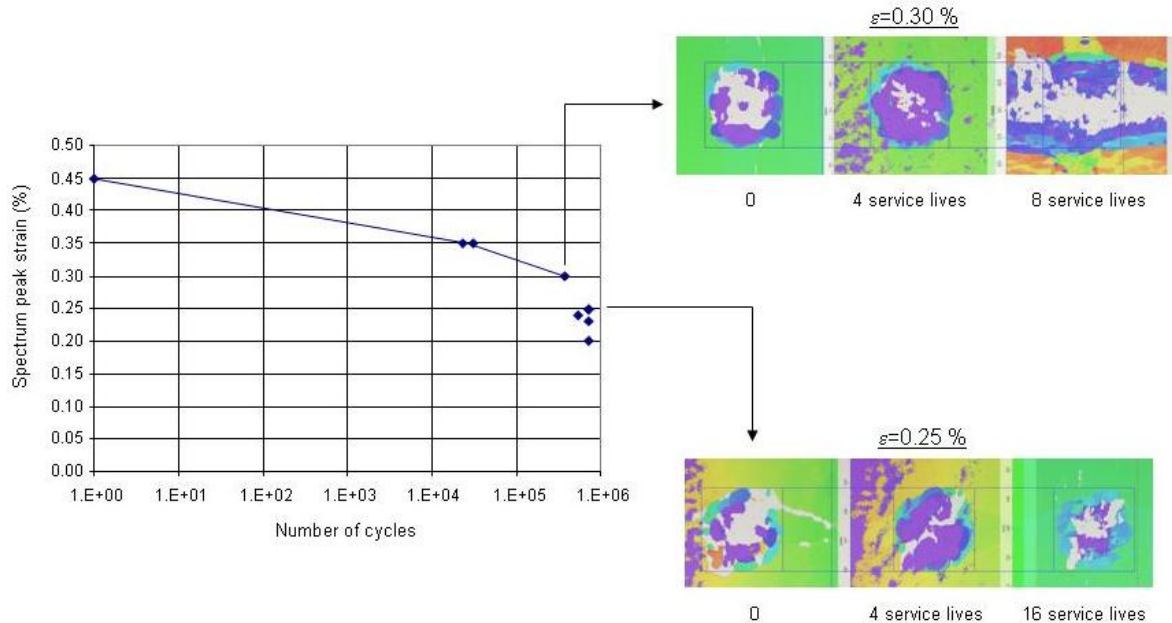


Figure 51. Fatigue test, damage development, and threshold value

### 3.5.3 Characteristics of Lamb wave in detecting damages in composite materials [9]

A systematic investigation has been performed concerning use of the characteristics of Lamb wave to detect impact as well as fatigue damages in composite laminates based on a network of PZT sensors. Thin PZT sensors are bonded on or embedded in composites specimens that are representative for aeronautical structures in high stressed locations. The PZTs are used both as the Lamb wave generators (actuators) and as Lamb wave receivers (sensors). The instrumented specimens have been subjected to various impact damages and fatigue loading after the impact damages, see figure 52. Various frequencies of Lamb wave, sizes of wave actuator and sensor, placements of PZT, and mounting techniques of PZTs have been studied. The investigation gives much insight about the use of Lamb wave in detecting damages in composite laminates. The results show that significant information about damage state may be obtained for the allowable impact damage and the fatigue propagation based on the characteristics of Lamb waves created using the PZT systems, when the right solution is identified. This research work is partly financed by European Union under the 6<sup>th</sup> framework in the project ARTIMA (Aircraft Reliability Through Intelligent Materials Application).

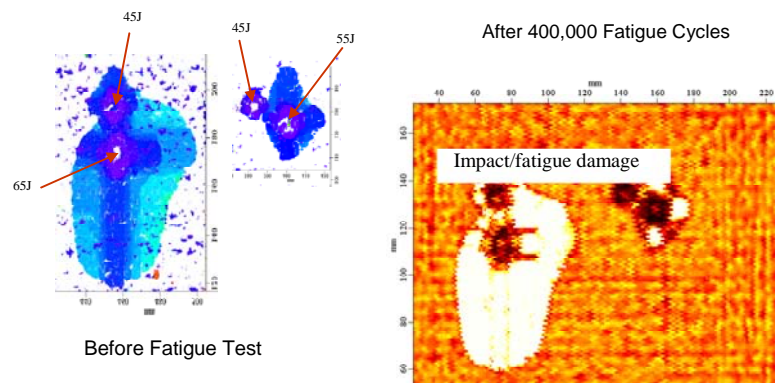


Figure 52. Comparison of damage before and after fatigue loading

Both experimental and numerical investigations (Figure 53) on the characteristics of Lamb wave propagation in the carbon fiber composite laminates have been performed for detection of the impact damage and fatigue damage in the laminates. This investigation shows that the Lamb wave, once excited in the composite plate, may be used to uncover small changes in the material due to damage or fatigue through the measurements in the change of characteristics in the

wave propagation, see FFT results of the signal shown in Figure 54. It is, however, a very difficult task to understand the information and to correlate the information to diagnose state of the material.

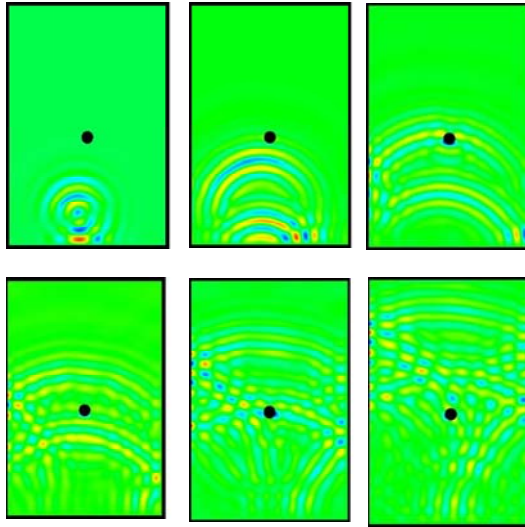


Figure 53. Simulated Lamb wave propagation in the test panel

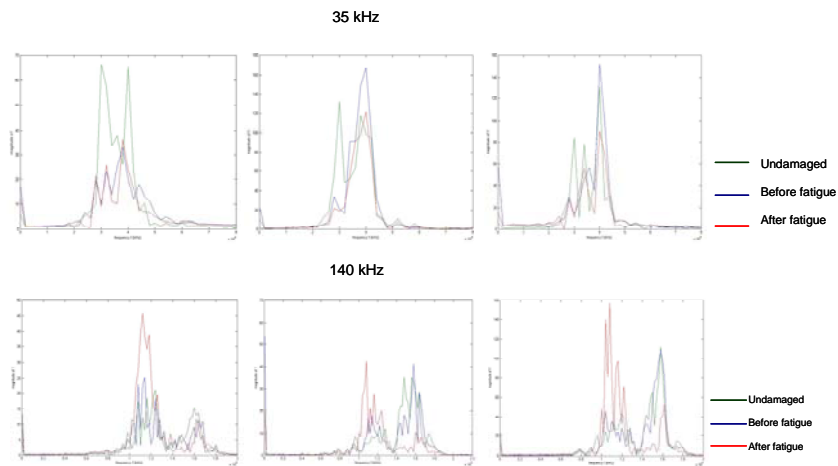


Figure 54. FFT of signal for various states.

### 3.6 REFERENCES

- [1] ICAF Doc.No 2411. A review of aeronautical fatigue investigations in Sweden during the period June 2005 to April 2007. Edited by Ansell, H. Presented at the 30th Conference of the International Committee on Aeronautical Fatigue (ICAF), Naples, Italy, 14-15 May 2007.
- [2] Ansell, H., Blom A.F. Structural life response in fighter aircraft due to systems command and control. Presented at the First International Conference on Damage Tolerance of Aircraft Structures R. Benedictus, J. Schijve, R.C. Alderliesten, J.J. Homan (Eds.) © TU Delft, The Netherlands.
- [3] B. Andersson, A. F. Blom, U. Falk, and G. S. Wang, K. Koski, A. Siljander, J. Linna, A. Miettinen, K. Vaaraniemi, R. Lahtinen, A Case Study of Multiple-Site Fatigue Crack Growth in the F-18 Hornet Bulkhead, In Proc. 25th ICAF Symposium, "Bridging the Gap between Theory and Operational Practice, Ed. M. Bos, 2009.
- [4] ICAF Doc.No. 2418. A review of aeronautical fatigue investigations in Finland. May 2007 to April 2009. Edited by Siljander, A. Presented at the 30th Conference of the International Committee on Aeronautical Fatigue (ICAF), Rotterdam, The Netherlands, 2009.
- [5] G. S. Wang, "FOI DaToN 2024-T3 HSC Panel Tests", FP6 program DaToN: contract No. AST3-CT-2004-516053, DaToN – WD - WP 3.4 – 7.0/FOI, Swedish Defence Research Agency, October, 2008.
- [6] G. S. Wang, "Validation of Damage Tolerance Analytical Models", FP6 program DaToN: contract No. AST3-CT-2004-516053, DaToN – WD - WP 4.3 – 1.0 / FOI, Swedish Defence Research Agency, October, 2008.
- [7] François Brastel, Stress Intensity Factors for Multiple Surface Cracks, FOI-memo SE, July 2008, Swedish Defence Research Agency, Stockholm.
- [8] Cf paper C in "Survival estimation for opportunistic maintenance" by Johan Svensson (PhD thesis in Mathematical Statistics at Chalmers, Gothenburg (2007).  
<http://www.math.chalmers.se/Stat/Research/Preprints/Doctoral/2007/4.pdf> )
- [9] G. S. Wang, "Fatigue Test for Impact Damage Growth Threshold in Composite Laminates under Variable Amplitude Loading Condition", Oct. 2008, FOI Memo-2557, Swedish Defence Research Agency

### 3.7 ACKNOWLEDGEMENTS

This work was supported by Saab Aerosystems. The editor is also indebted to the following individuals who helped to write parts of this review:

Anders Blom	FOI	(Section: 3.4.1)
Anders Bredberg	SAAB	(Section: 3.5.1)
Henrik Elinder	SHK	(Section: 3.2.1)
Kristian Lönnkvist	SAAB	(Section: 3.3.8)
Lennart Magnusson	SAAB	(Section: 3.4.5)
Jaques de Mare	Chalmers	(Section: 3.4.6)
Stefan Thuresson	SAAB	(Sections: 3.2.2, 3.3.1, 3.3.2, 3.3.3)
Geng-Sheng Wang	FOI	(Sections: 3.4.2, 3.4.3, 3.4.4, 3.5.2, 3.5.3)
Urban Wendt	SAAB	(Section: 3.3.7)